AD-A115 551 AIR FORCE INST OF TECH WRIGHT-PATTERSON AFB OH SCHOO--ETC F/G 10/2
AC RESONANT CHARGING FOR INTERFACING PRIME POWER TO PULSE CONDI--ETC(U)
DEC 81 W C DUNGAN
UNCLASSIFIED AFIT/GE/EE/81D-18 NL

END
DATE FILMED
7 82
DTIC

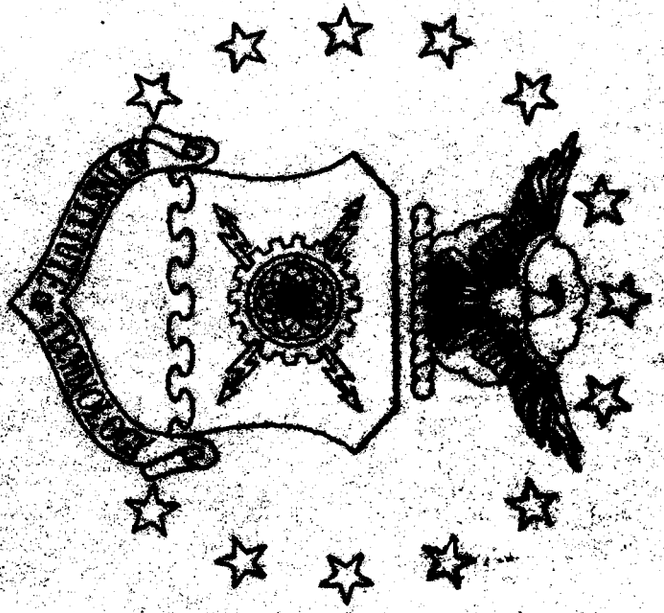

AFIT/GE/EE/81D-18

AC RESONANT CHARGING FOR INTERFACING PRIME POWER TO PULSE CONDITIONING CIRCUITS

THESIS

AFIT/GE/EE/81D-18 William C. Dungan
Capt USAF

AFIT/GE/EE/81D-18

AC RESONANT CHARGING FOR INTERFACING PRIME POWER TO PULSE CONDITIONING CIRCUITS

THESIS

Presented to the Faculty of the School of Engineering

of the Air Force Institute of Technology

Air University

in Partial Fulfillment of the

Requirements for the Degree of

Master of Science

by

William C. Dungan, B.S.

Captain USAF

Graduate Electrical Engineering

December 1981

Preface

This thesis project has been one of the most challenging experiences I have encountered. I am grateful to Dr. Frederick Brockhurst for introducing me to the AC resonant charging topic and to Dr. Robert Fontana and Capt. Tim Skvarenina for their counsel after Dr. Brockhurst's retirement from the Air Force.

Before entering AFIT I was fortunate enough to visit the Electric Power Laboratory at MERADCOM. I was quite impressed with the personnel, facilities, and general work philosophy and tried to get an assignment into the organization. Though this was not possible it did open the door for this research project which was conducted at MERADCOM's Electrical Equipment Division. Quite a number of people in this organization supported this thesis effort. I am grateful to them and especially to my advisors Dr. Alois L. Jokl, Dr. Larry I. Amstutz, and Dr. James Ferrick and also to Mr. Michael Mando. Each of these individuals played a unique and invaluable role during the research process. Their knowledge, experience, and professionalism was tinted with enough empathy to gain for them my deepest respect. I would also like to thank Mr. Carl Heise for providing me with needed expertise on machine theory and Mr. Bobbie Browning and Mr. Gerald Sullivan for their assistance during the experimental tests.

I am also appreciative of the enthusiastic support given this study by Mr. James P. O'Loughlin of the Air Force Weapons Laboratory and Dr. Richard W. Gilchrist of Clemson University. These individuals provided both stimulating discussion and advice on sidestepping a number of pitfalls. Finally, a special thanks goes to my wife, Donna, for her help and understanding during this study.

William C. Dungan

Contents

Contents

List of Figures

List of Tables

Abstract

The impact on a prime power source due to AC resonant charging was investigated. The source was a standard DOD 15 KW, 400 Hz alternator. Adverse impact on the alternator was almost negligible for a varying load of 15 to 60 KW and a frequency change of 380 to 475 Hz. The only exception was caused by the pulser diodes. Their turn-on was reflected in the alternator voltage waveforms. An indirect approach is presented for determining resonance and, thus, the internal reactance contribution by the alternator. This value was found to be slightly less than that specified for the leakage reactance. The investigation concludes that resonance, in the classical steady state sense, is never reached. Even though the charging circuit has a transient response, the alternator armature reaction is approximately fixed. This implies that the alternator is in a near steady state mode of operation.

AC RESONANT CHARGING FOR INTERFACING PRIME POWER TO PULSE CONDITIONING CIRCUITS

I. Introduction

Background

The advent of directed energy weapons has spurred the development of a large number of supporting technologies. Two of these are the power source and power conditioning. The development of these technology areas has been driven by several factors. Primary among these are the beam weapon's inefficiency (requirement for high power), voltage and current waveshaping (requirement for advanced power conditioning), and dependable interfacing of the power source with the power conditioning equipment (requirement for lightweight, low volume charging of the intermediate energy store). The last of these is the topic of concern for this research effort.

The Army and Air Force are both concerned with the interface problem and have expended considerable resources toward its resolution. The Army's need stems from the requirement for systems that are ground mobile. Thus, all equipment in this general category must be relatively light and low volume. The Air Force requirements are even more stringent since its systems must be flyable.

One possible way to resolve the interface problem is by the use of AC resonant charging. This method employs an AC voltage source to recharge the energy storage condenser of a voltage-fed network. It has been the subject of only a small number of tests. Thus, there is only limited information (and understanding) concerning the interface between the alternator and the charging system during its use.

In 1976 Airesearch Manufacturing Company submitted their findings for the AC resonant charging tests they had performed on a modified alternator (Ref 9). One of the secondary objectives of the program was to test the machine and its loading circuit at precise resonant conditions. Although this objective was not met, the machine was tested at two different off-resonant conditions. This study was sponsored by the Air Force Weapons Laboratory (AFWL). The AFWL also sponsored the 1978 Power Generation Study and Test Program which was conducted by the Mobility Equipment Research and Development Command (MERADCOM), Ft. Belvoir, Virginia. Among other conclusions, it found that including all of the AC resonant charging inductance inside the alternator was not only feasible but could also provide an overall weight saving for the system. Most of the charging inductance is normally included in a high leakage transformer.

The latest effort involving AC resonant charging is a program being conducted by Clemson University and sponsored by the Aero Propulsion Laboratory at Wright-Patterson AFB, Ohio. The Clemson investigators are developing computer simulations which are designed to predict the internal inductance of the power source during the AC charging mode. Thus, the results of this thesis research effort should serve as a weighted input to either refine or validate the Clemson predictions.

Problem and Scope

The major problem was the lack of a full understanding of the interaction of the alternator with the remainder of the charging circuit during the AC resonant charging mode. The impact on the alternator needed to be determined for varying loads and frequencies. It was believed that this mode of operation did not have the same adverse impact on the alternator

as did DC resonant charging (Ref 8:50). However, this needed to be confirmed. Also, an investigation needed to be made to determine what actually constitutes resonance, when does it occur, and when it does occur what is the effective internal machine reactance. To gain a fuller understanding of the charging system, attention also had to be given to the discharge circuit, system grounding (loops), system noise, pulse triggering, and the physical layout of the pulser. Thus, the study was primarily concerned with the charging system and minimal effort was devoted to other system aspects such as the discharge circuit.

Approach

The first step in this investigation was a review of AC resonant charging theory. The equations derived theoretically were then consolidated into a computer program called EQUATE that developed the data needed to provide plots of the circuit voltages and current. Following this the Runge-Kutta programs RLCCHG and RLCDIS were written to integrate the differential equations of the charge and discharge circuits, respectively. These latter programs solved the system equations for all frequencies while program EQUATE was applicable only at the circuit resonant frequency. Once these theoretical models were developed, the experimental effort began. The system was configured and tested at 15, 30, 45, and briefly, at 60 kilowatts. Special tests were also made in order to determine resonance and, thus, the effective machine reactance.

Sequence of Presentation

A detailed description of AC resonant charging theory is presented in Chapter II. Chapter III describes the experimental results and their analyses. The project conclusions and recommendations for future study

are presented in the final chapter.

There are also five appendices. Appendix A presents a detailed development of the half cycle charging equations. Appendix B provides a listing of program EQUATE. Appendix C includes the operating instructions for developing programs which will use the subroutine RKFOUR. It also provides a listing of RKFOUR, RLCCHG, and RLCDIS. Appendix D contains a list of the test equipment. The last appendix gives the results of the leakage transformer short-circuit test.

II. Theory of AC Resonant Charging

While the theory of AC resonant charging has been known for at least the last four decades it has yet to receive thorough publication coverage. The "grandfather text" is Pulse Generators (Ref 2) which was edited by Glasoe and Lebacqz shortly after World War II. The following material is a brief synopsis taken from this text.

The Pulser

The circuit that delivers the pulses of energy to a load is referred to as a "line-type pulser." This type of pulser discharges all of its energy during each pulse. The scope of this presentation does not cover the "hard-tube pulser" which delivers only a small fraction of its stored energy into the load during a single pulse. Generally, the discussion of a pulser can logically be divided into two categories, the charge and discharge circuits. This is possible since the charging of the energy-storage component of the pulser requires a time that greatly exceeds the discharge time. The discharge circuit will be introduced. However, this presentation will be directed primarily at the charging circuit.

The Discharge Circuit

The basic discharge circuit of a pulser can be represented schematically as shown in Figure 1. If the energy for the pulse is stored in the electrostatic field of a capacitor(s), then the unit is a "voltage-fed network" as opposed to a "current-fed network" which stores its energy in a magnetic field. This energy storage device is often referred to as a "pulse-forming network" or PFN. "When the load impedance is equal to the characteristic impedance of the network, assuming the switch to have negligible resistance, all the energy stored in the network is transferred

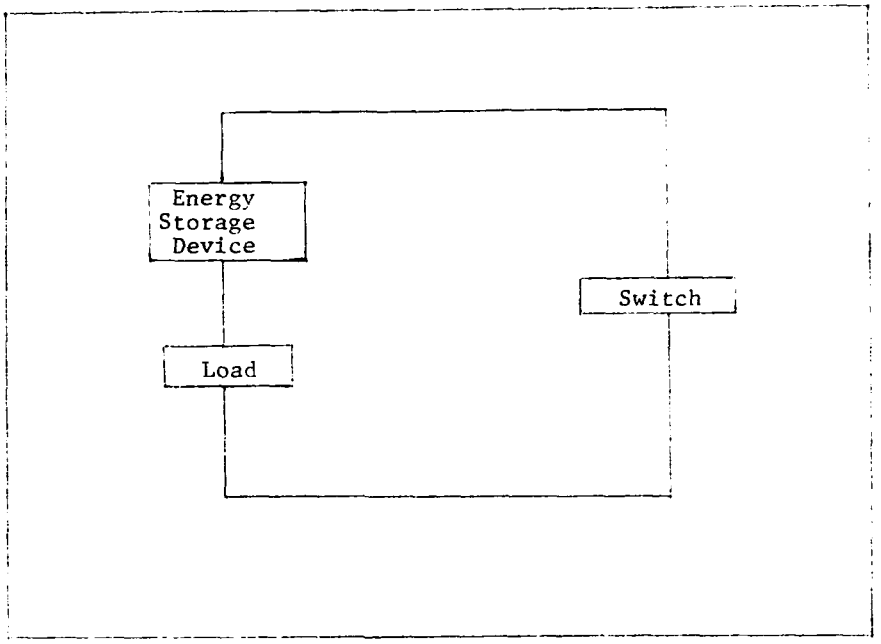

Figure 1. Typical Discharge Circuit of a Pulser

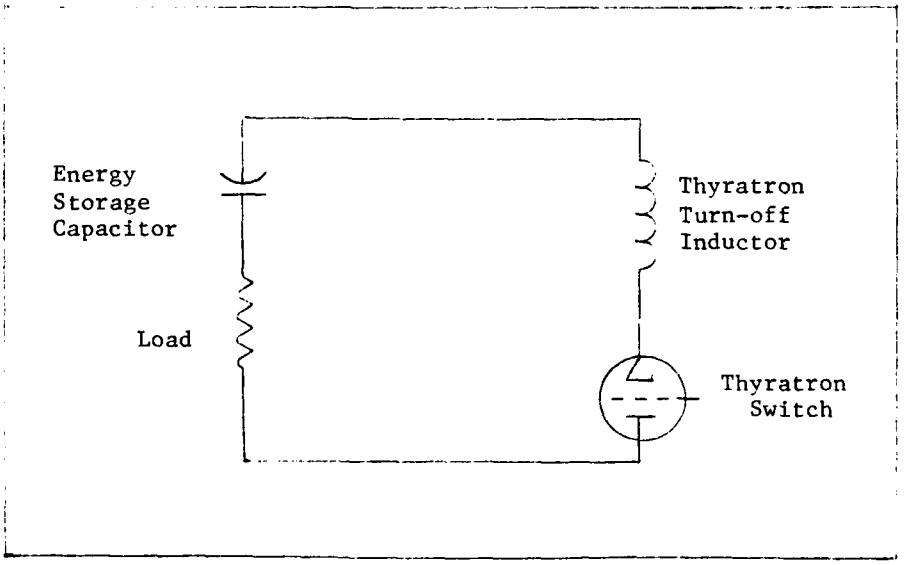

Figure 2. Simplified Discharge Circuit for the MERADCOM Pulser

to the load, leaving the condensers in the network completely discharged" (Ref 2:8).

A simplified schematic for the pulser discharge circuit built for the MERADCOM facility is shown in Figure 2. A single capacitor is used as the energy storage device and, thus, the circuit does not truly contain a PFN. The load is an eleven ohm resistor and a thyratron is used for switching. A small inductance has been placed in the series loop in order to drive the thyratron anode voltage to a slightly negative value which assures turn-off of the switch. Therefore, all of the available energy is not discharged to the load. A very small amount is returned and negatively charges the energy storage capacitor. This process, however, does not consume energy but rather slightly reduces the amount which can be used by the load.

The Charging Circuit

Resonant charging of a voltage-fed network in a line-type pulser can be accomplished in several ways. For example, one of the best known methods is to use a DC power supply. This approach was studied by Lt. Jaime Silva who noted that it presented a number of problems, namely, "vibration of the generator at the pulse repetition rate, irregular voltage and current waveforms in the generator, and lower performance of the DC resonant circuit due to input voltage sag" (Ref 8:50). However, a system based upon this method is relatively simple in its construction and triggering features.

Resonant charging may also be realized using an AC power supply. Though more complicated, this approach has a number of advantages over DC resonant charging. As concluded by Lt. Silva, this latter charging scheme is not expected to cause a negative impact upon the power source.

However, it does require that the AC source frequency be integrally related to the pulse recurrence frequency (PRF). This is necessary since the charging period must terminate at a current zero crossing. As there are only two zero crossings per cycle, the PRF must not be greater than twice the AC frequency. The relationship between the PRF and the AC frequency is given by the following equation.

$$PRF = \frac{2}{K} f_{AC} \qquad (1)$$

where

$K = 1,2...$

f_{AC} = impressed AC frequency

A value of K = 1 corresponds to half cycle charging and K = 2 to full cycle charging. If the PRF is twice the AC frequency then the network voltage attains a value approximately $\pi/2$ times the peak AC voltage. Though this fixed frequency requirement allows little flexibility in the alternator-pulser interface, the deficiency is offset somewhat by the advantage of being able to control the pulse power output by varying the alternator field current. Another advantage is that this system permits a net saving in weight and size relative to the DC system. Its block diagram is shown in Figure 3.

There are a number of requirements levied upon this circuit. Among them is the need for high efficiency. This normally eliminates the use of a resistor for the charging element since its inherent efficiency can never exceed 50 per cent. The charging element must allow the discharge of the network at a peak voltage. It must also be capable of isolating the source from the time the switch closes until it deionizes (for a gaseous switch). For example, if the network is connected directly to

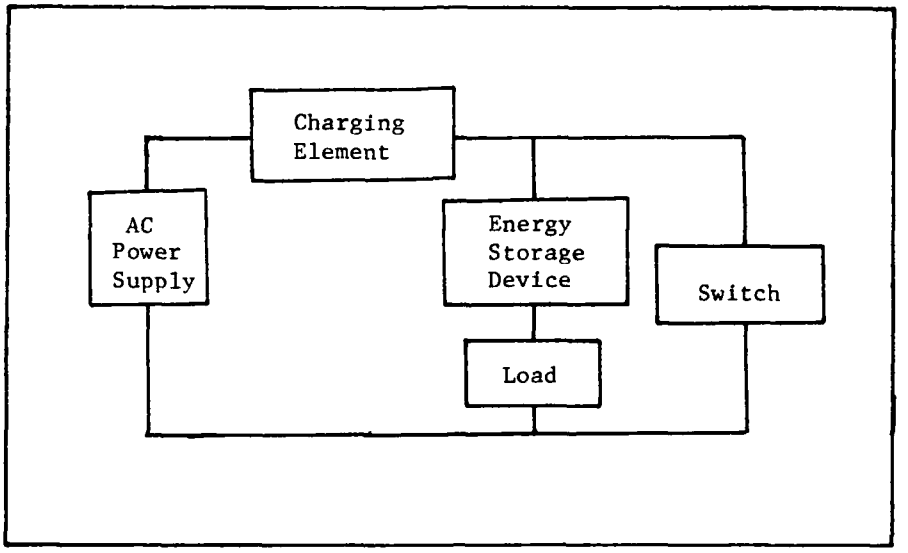

Figure 3. Block Diagram for the Complete Pulser Circuit

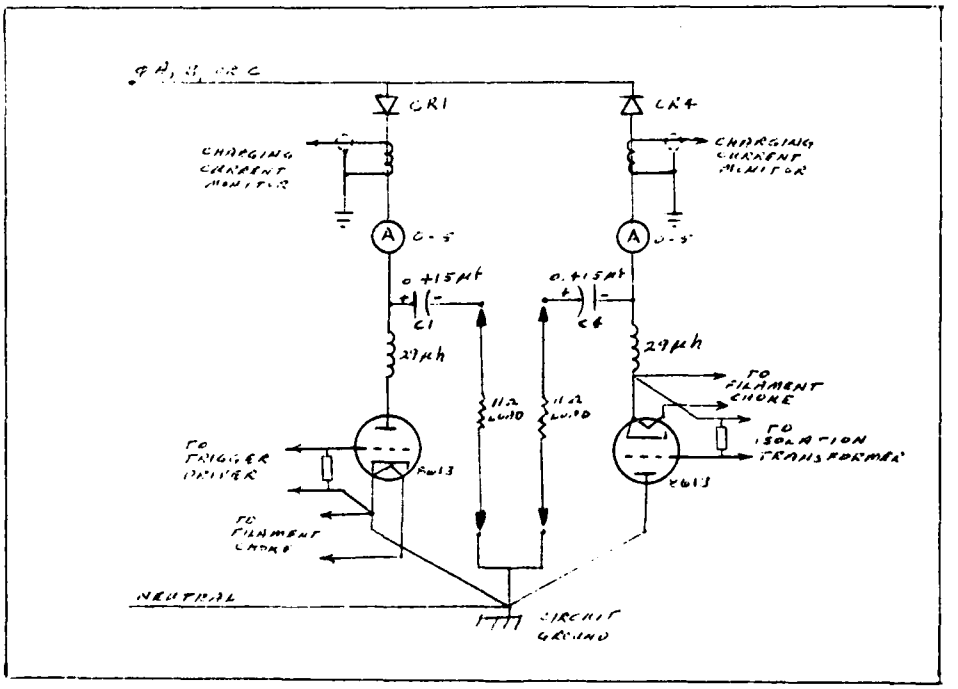

Figure 4. Schematic Diagram of the MERADCOM Pulser

the high voltage terminals of a transformer and discharged at a voltage peak, the network begins to recharge immediately, the switch fails to re-open, and the transformer is short-circuited for the remainder of the half cycle.

This problem may be avoided by placing a hold-off diode between the high voltage transformer and the energy storage network. Figure 8 shows such an arrangement. The network (capacitor) may now be discharged during the following half cycle which has a polarity opposite to that of the charging half cycle. This provides stable circuit action and eliminates the problem associated with the continual build-up of the charging voltage and current should the discharge circuit switch fail to operate (close). As shown in Figure 8, all phases have two charging circuits and each of these contains a hold-off diode. One circuit network is charged during a positive half cycle and the other is charged during a negative half cycle. The transformer utilization factor is greatly improved by this approach.

The MERADCOM Pulser

These advantages are incorporated in the circuit of Figure 4. This circuit is the basis for the MERADCOM pulser. It provides a more detailed account of one of the phase networks of Figure 8. A description of its operation will now be presented.

During the positive half cycle capacitor C1, the energy storage device, is charged. The voltage on C1, V_{C1}, reaches its peak when the source (alternator) voltage and charging current pass through zero. V_{C1} remains at this peak value for a brief time into the negative half cycle. When the source voltage reaches a specified negative value a trigger pulse is sent to the thyratron in the C1 discharge circuit. The thyratron

fires and discharges the stored energy into the 11 ohm resistive load. As the discharge current tends to zero, the voltage on the small inductor at the switch anode reverses polarity. This forces a slight negative charge on C1 which assures proper turn-off of the thyratron. During the negative half cycle the source charges C4 and the same chain of events occur as described for C1.

General Approach to the Theoretical Analysis

Independent theoretical analyses were performed on both the discharge circuit and the charge circuit of the pulser. A number of computer programs were developed. These divide into two general categories as implied in the introduction. The first of these was simply an application of the AC resonant charging equations derived in Appendix A. These equations were used to show how the circuit current and voltages varied over a half cycle of charging. However, their use was applicable only to a circuit operating at the resonant frequency. This program of equations is listed in Appendix B as Program EQUATE.

The second program category was based upon the use of a Runge-Kutta integration subroutine called RKFOUR which was developed by B. D. Weathers. Programs were developed, following his suggested format, that would integrate the differential equations for a number of cases. The most useful of these were Program RLCCHG and Program RLCDIS which integrated the charge and discharge circuit equations, respectively. Program RLCDIS was obtained by slightly modifying Program RLCCHG. Both of these programs, as well as RKFOUR and instructions for its use, are listed in Appendix C. They each integrate their respective circuit equations over a half cycle. Program RLCCHG was found to be particularly useful since it, in contrast to Program EQUATE, is capable of integrating the charging circuit equations

at off-resonant frequencies.

Theoretical Analysis of the Discharge Circuit

As noted earlier, the discharge circuit for the MERADCOM pulser can be represented by the schematic shown in Figure 2. The differential equations for this circuit were integrated using Program RLCDIS with the resistance of the switch neglected. The current and voltage curves shown in Figures 5 and 6 resulted from the selection of a 0.43 μf capacitor, an 11 ohm load resistor, and a 29 μh inductor. The capacitor was

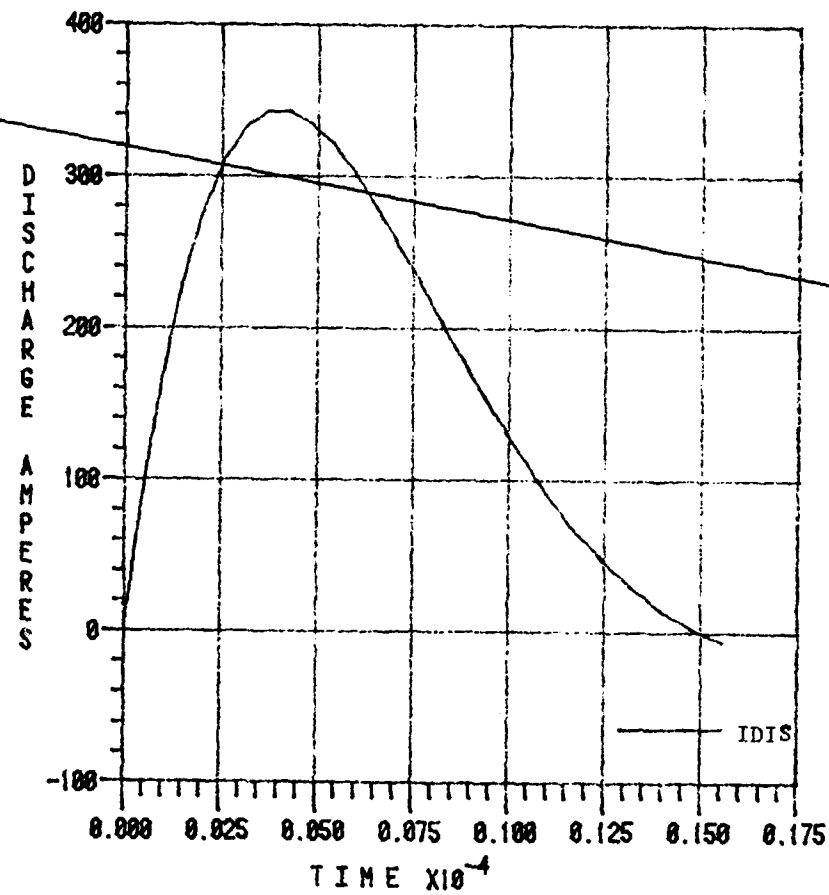

Figure 5. Pulser Discharge Current Using Program RLCDIS

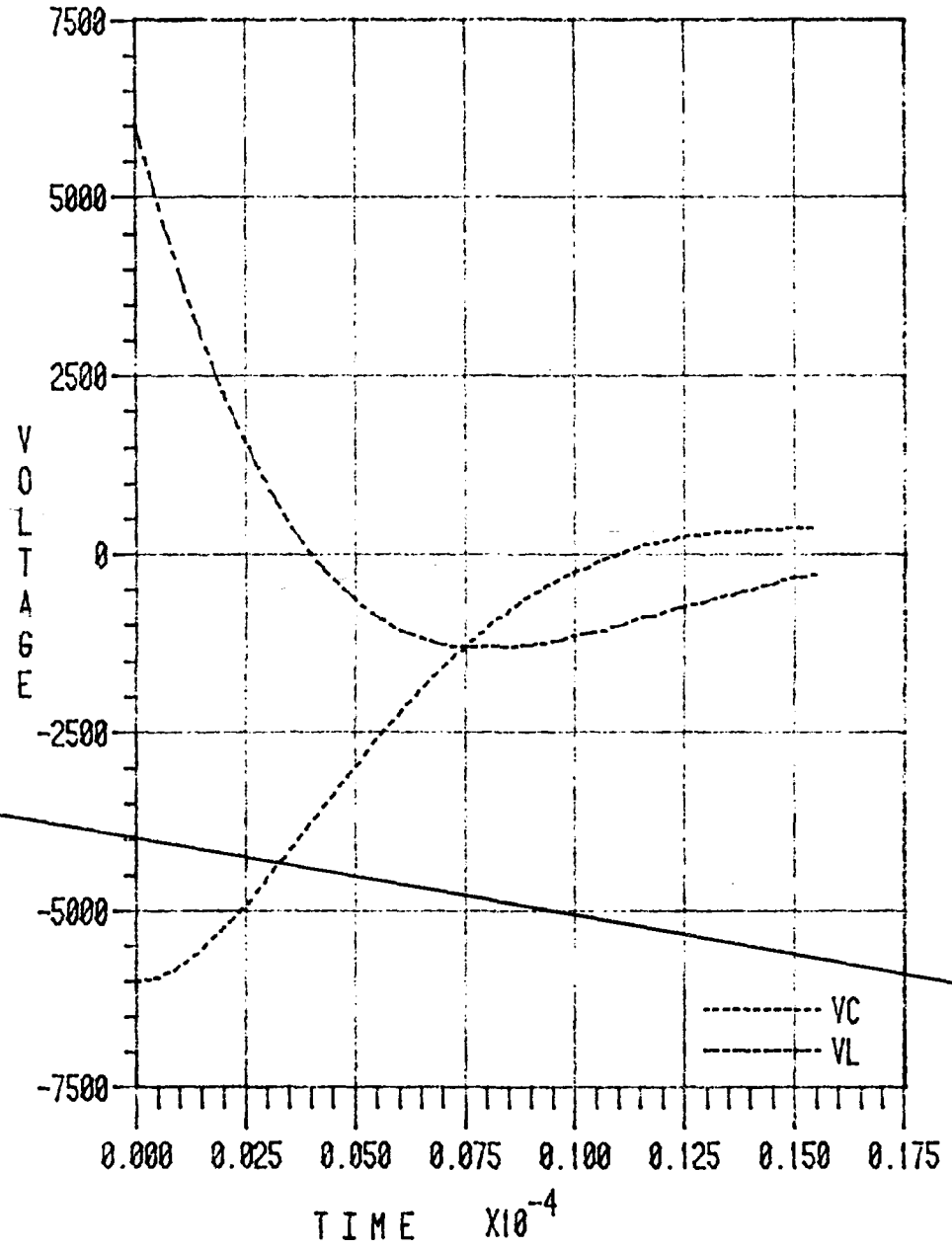

Figure 6. Discharge Circuit Capacitive and Inductive Voltages Using Program RLCDIS

initially charged to -6000 volts. This value was read from the oscillograms for a load of approximately 20 KW. As seen in the curves, at the time of the current zero crossing the capacitor voltage has reversed its polarity. This reverse charge forces the thyratron switch to turn off. Thus, the discharge circuit is isolated from the charging circuit throughout the interpulse period.

Theoretical Analysis of the Charging Circuit

Figure 7 shows the simplified schematic for the circuit used in half cycle AC resonant charging. The more detailed three phase representation of the MERADCOM circuit is shown in Figure 8.

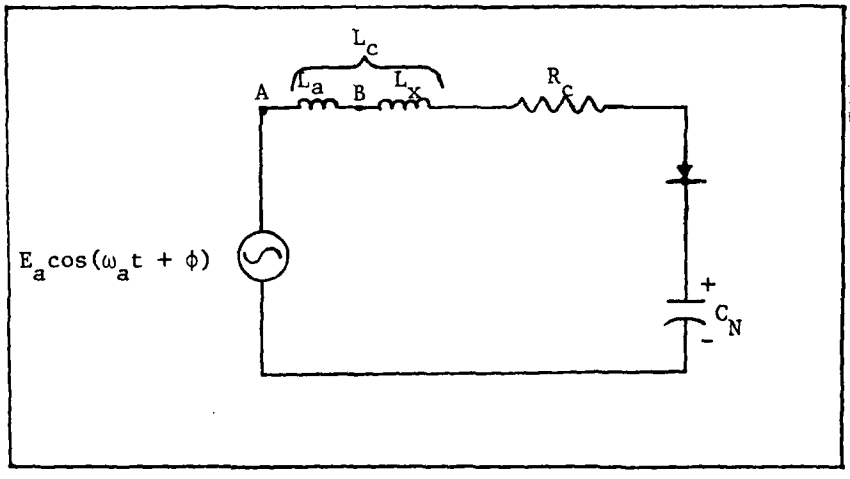

Figure 7. Simplified Circuit for Half Cycle Charging

The mathematical analysis for the circuit of Figure 7 is given in Appendix A. The charging inductance, L_c, is made up of the internal machine inductance, L_a, and the large transformer leakage inductance, L_x. The charging resistance, R_c, is the series combination of the source internal resistance, the transformer resistance, and the load resistance.

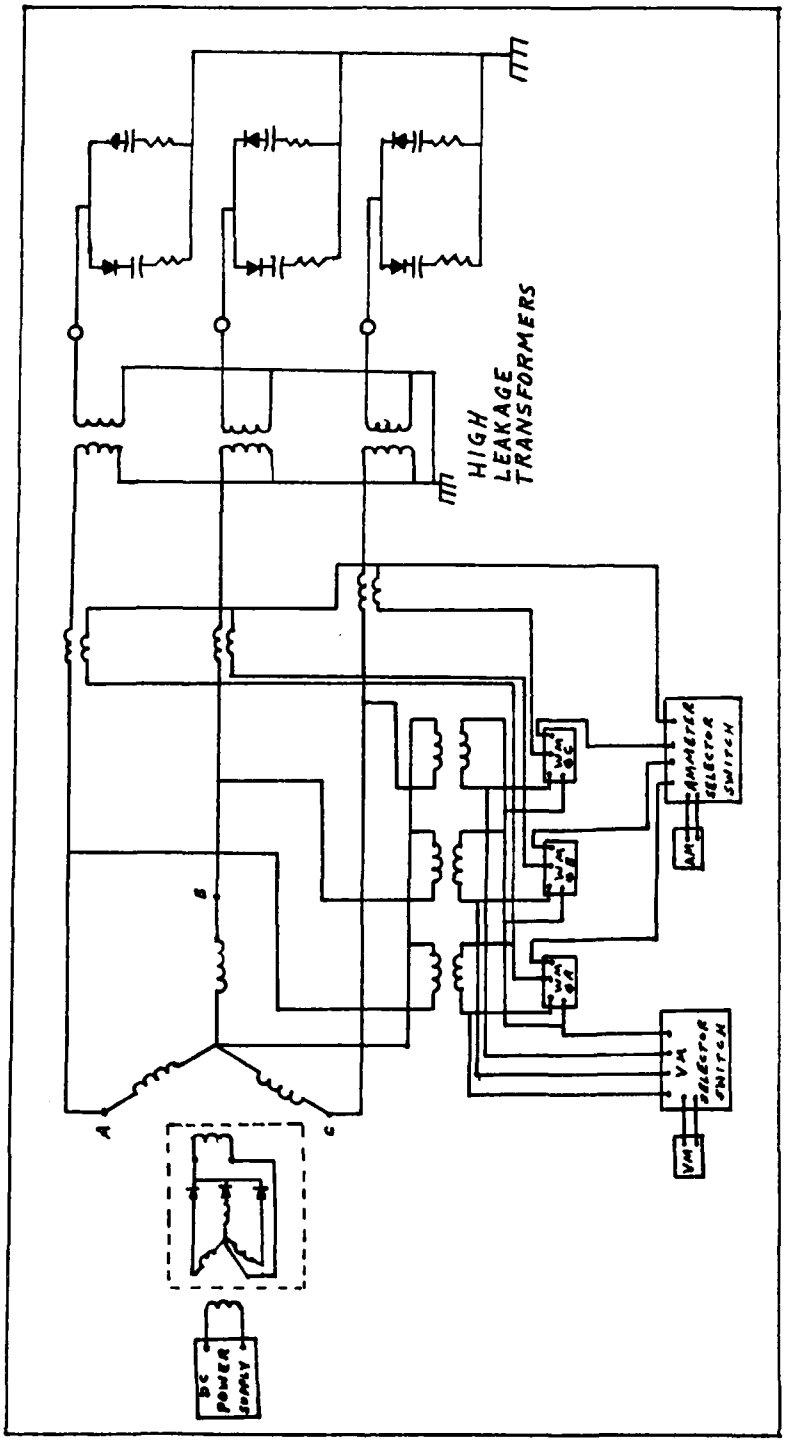

Figure 8. Charging Circuit for the AC Resonant Mode

C_N is the fixed capacitance of the energy storage device.

From Appendix A it was determined that C_N charged up to its maximum voltage when the power source phase angle was equal to $-\pi/2$. Using this value and recognizing that $q_N(0) = C_N v_N(0)$ the following expressions for the charging current and the circuit voltages may be obtained (see Appendix A)

$$i_c(t) = QC_N E_a \omega_a \{(1 - \varepsilon^{-\frac{\omega_a t}{2Q}}) \sin\omega_a t - \frac{v_N(0)}{QE_a} \varepsilon^{-\frac{\omega_a t}{2Q}} \sin\omega_a t\} \quad (2)$$

$$v_N(t) = Q\{(\varepsilon^{-\frac{\omega_a t}{2Q}} - 1)\cos\omega_a t + \varepsilon^{-\frac{\omega_a t}{2Q}} [\frac{v_N(0)}{QE_a} \cos\omega_a t + (\frac{1}{2Q} + \frac{1}{2Q^2} \frac{v_N(0)}{E_a}) \sin\omega_a t]\} \quad (3)$$

$$v_L(t) = E_a \sin\omega_a t - i_c(t) R_c - v_N(t) \quad (4)$$

where

$Q = \frac{\omega_a L_c}{R_c}$, the quality factor of the circuit

E_a = peak emf generated inside the alternator (volts)

ω_a = the natural resonant frequency (radians/second)

$v_N(0)$ = the initial capacitor voltage (volts)

$v_L(t)$ = the voltage across the inductor (volts)

Equations (2)-(4) may now be plotted versus time. When this is done with Program EQUATE the curves in Figures 9 and 10 result. Figure 9 closely resembles the typical tsint curve. This form is evident in the simplified expression for the charging current. For example, with $i_c(0) = 0$, $\phi = -\pi/2$, and $q_N(0) = C_N v_N(0)$, equation (A-22) becomes

$$i_c(t) = \frac{E_a t}{2L_c} \sin\omega_a t - \omega_a C_N v_N(0) \sin\omega_a t$$

or

$$i_c(t) = [\frac{E_a}{2\omega_a L_c} \omega_a t - \omega_a C_N v_N(0)] \sin\omega_a t \qquad (5)$$

For zero initial charge on the capacitor or for a small charge using typical circuit values, the second term in the above equation can be neglected. The curves of Figures 9 and 10 were plotted with $R_c = 0.445$

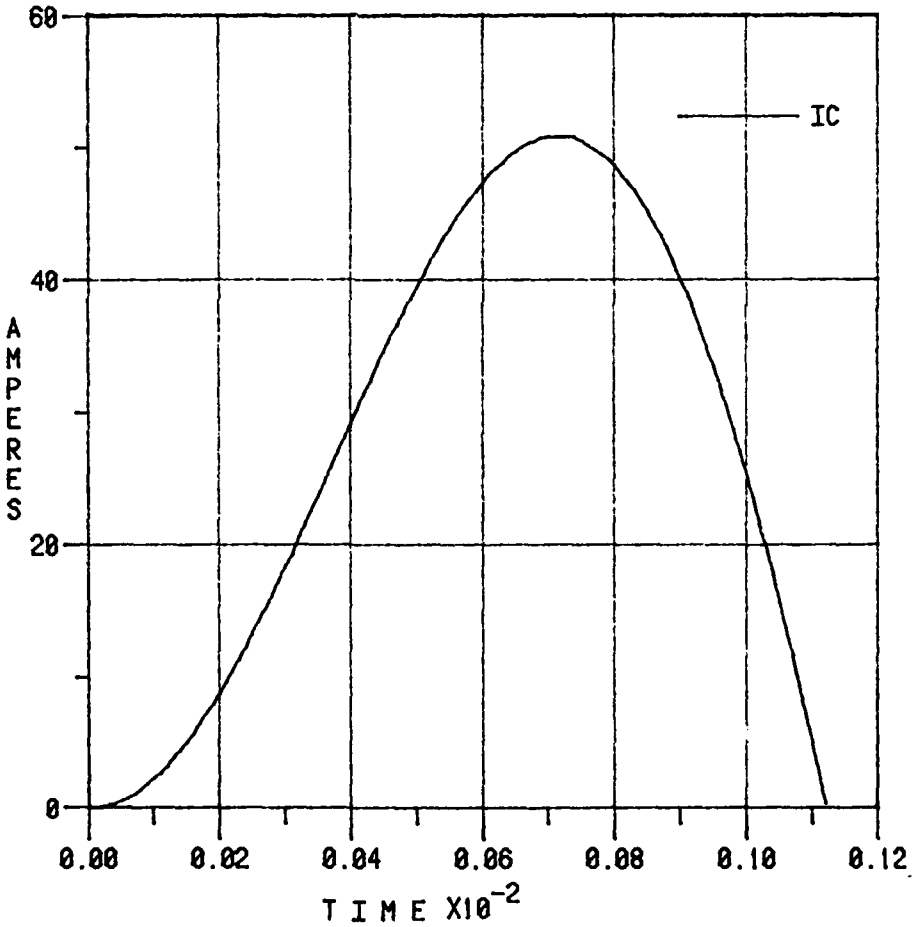

Figure 9. Charging Current for the MERADCOM Pulser Using Program EQUATE.

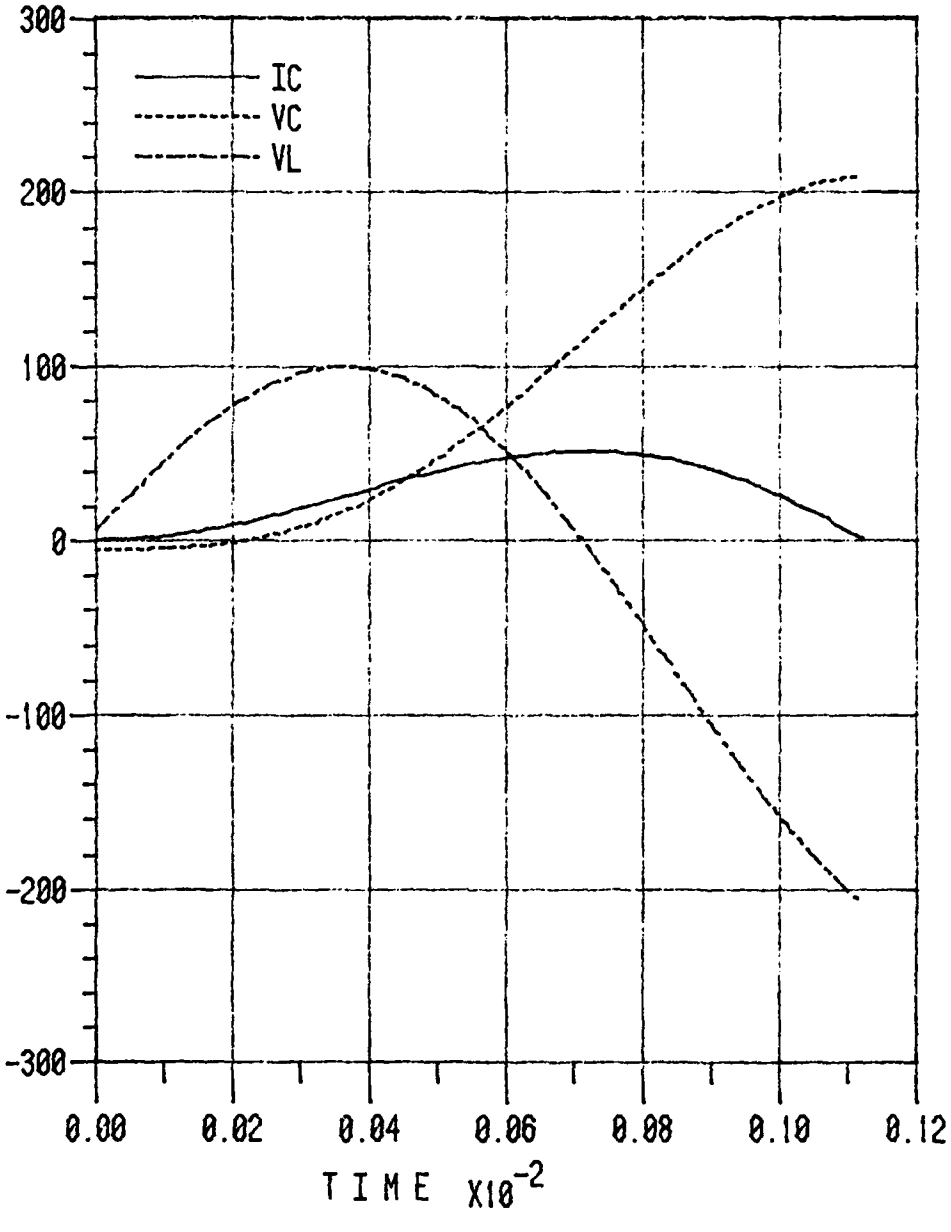

Figure 10. Charging Current, Capacitor and Inductor Voltages for the MERADCOM Pulser Using Program EQUATE

ohms, C_N = 147 μf, $v_N(0) = -5.4$ volts, E_a = 150 volts, and L_c = 0.858 mh. These values were selected early in this study. Their substitution into equation (5) yields

$$i_c(t) = (87413t + 1.99)\sin 2802t \qquad (6)$$

The Results section will show that the above values are not very different from the final values which were either measured or calculated.

With the exception of the first 22 microseconds, the complete half charging cycle (1.12 msec) is dominated by the first term in equation (6), that is, the $\omega_a t \sin \omega_a t$ term. Since the charging voltage $v_N(t)$ is a function of the integral of the current it will reach its maximum value at the end of the charging half cycle (π radians). Again, the purpose of the diode in Figure 7 is to block the circuit's attempt to lower this voltage after it has reached its peak value. Without the diode the current would go negative at the end of the half cycle. This would cause a reverse polarity on the capacitor which, at the end of a full cycle, would be twice the half cycle value. This is known as full cycle charging. Without proper controls the voltage could, as explained earlier, build up to a dangerous level, especially should the discharge switch fail to operate. With half cycle charging this disadvantage is eliminated.

III. Results and Discussion

The circuit of Figure 8, with the discharge switch branch included, was set up and testing was begun. However, the circuit was later partially disconnected to confirm the resistance, inductance, and capacitance values of the major components. These components are listed in some detail in Appendix D. The per phase DC resistance of the alternator was found to be approximately 0.18 ohms. This value was multiplied by a factor of 1.5 to account for the resistive change due to loss mechanisms such as hysteresis and eddy currents (Ref 4:255; 5:227-237). A short circuit test of the C phase high leakage transformer was then conducted. The results of this test are recorded in Appendix E where all values are referred to the low voltage side of the transformer. The resistance and inductance (at 400 Hz) were found to be 0.1427 ohms and 0.690 mh, respectively. Also, a capacitance of 0.415 μf was measured for one of the energy storage (charging) capacitors. Since these tests were not performed initially, some of the earlier theoretical analyses (plots, for example) were based on slightly different nominal component values.

System Grounding and Noise

During the early stages of testing the pulser system was found to be inherently noisy. It was this problem that restricted Lt Silva's operation of the system to a low power level. His report indicates that multiple trigger signals prevented the build-up of voltage on the charging capacitors and that this malfunction was caused by the electronic logic circuit (Ref 8). He did not have sufficient time to diagnose this problem. However, after his departure the MERADCOM engineers discovered that

one of the wires which fed the trigger pulse to a thyratron switch was positioned too close to one of the discharge circuit cables. Such close proximity allowed each discharge in the cable to cause a corresponding noise pulse in the thyratron trigger circuit. Thus, the noise from one discharge circuit caused the inadvertent discharge of another circuit. The charging circuit inductance isolated the power source during this positive half cycle transient. Such isolation is normally needed only during the negative half cycle since the storage capacitors are discharged during this period of time. The hold-off diodes perform this isolation function.

The physical layout of the pulser complemented the noise problem by causing a number of ground loops. Initially, there were ground ties at the front, rear, and sides of the pulser structure. With certain measurements this caused no problems. However, some measurements could not be taken simultaneously with the dual trace scope. For example, it was not possible to initially measure the charging current and charging voltage at the same time. The charging current measurement was obtained by use of a current transformer which was grounded at the right end of the structure. The ground for the charging voltage was located at the front of the structure. When these two grounds were tied together at the scope inputs, the display of the charging current waveform was very distorted. The system was improved somewhat by either removing (as in the case of the charging current ground) or relocating (as with the charging voltage ground) certain ground connections.

It quickly became evident that considerable improvement could have been made in the shielding, grounding, and physical layout of the pulser. It would be difficult to correct these deficiencies now that the pulser

has been constructed. Hindsight suggests, as usual, that they should have been made during the design.

The Discharge Circuit

Though the discharge circuit was not studied thoroughly, its current waveform was viewed on the oscilloscope in order to make a theoretical comparison. By integrating the equations for the simplified discharge circuit of Figure 2 the discharge current waveform of Figure 5 was obtained. The small thyratron turn-off inductance of the circuit was initially measured to be approximately 51 μh. This caused the post-discharge voltage on the capacitor to reach an abnormally high level (approximately 800 volts). Reducing the inductance to 29 μh by tap adjustment caused this voltage to decrease to a value less than 300 volts. Since this value of voltage was quite sufficient for turning the thyratron off, it was used as an integral coefficient in the development of the curve in Figure 5. This curve may be compared with the measured discharge current curve of Figure 11.

These waveforms are quite similar and some of their differences can be readily explained. For example, the calculated current peak approaches 340 amps whereas the measured current peak is only 300 amps. Some reasons for this difference may be the use of a 0.43 μf capacitor in the calculations while its measured value was found to be 0.415 μf, the neglecting of all circuit resistance except the load, and the inclusion of only the thyratron turn-off inductance. Each of these modeling assumptions tend to increase the calculated current peak. Also, the computer program selection of an initial capacitor voltage of 6000 volts was based upon a scope reading that could well be off by 5%.

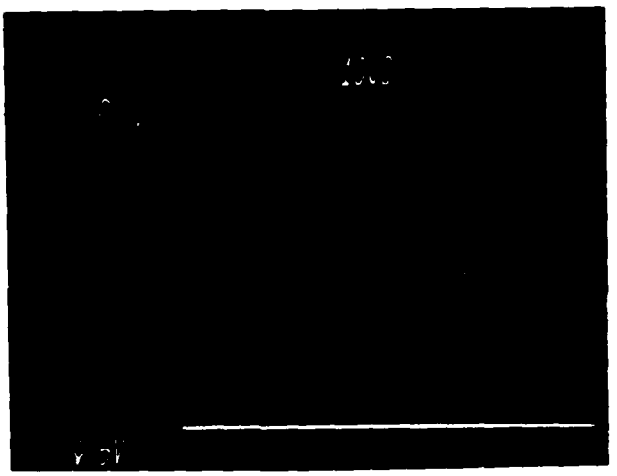

Figure 11. Pulser Discharge Current (50 amps/div, R = 11 ohms, C = 0.415 μf, L = 29 μh, $V_c \simeq$ 6000 volts)

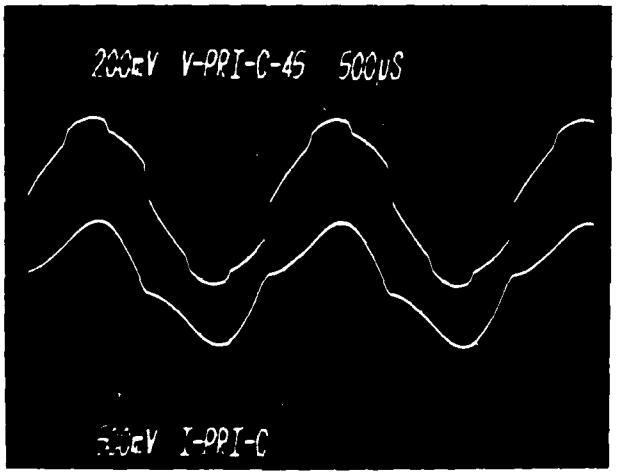

Figure 12. Primary Current and Voltage at the Alternator Terminals

The second difference in the waveforms is in the time to the current zero crossing. The calculated waveform shows a half period of only 15 μsec while the experimental value approaches 19 μsec. Correcting the capacitance to the smaller value tends to decrease the calculated half period even further. However, an increase in the circuit resistance and inductance due to the various components, such as the thyratron, tend to increase the half period. Thus, a correction in the circuit resistance and inductance appears to override the slight change in capacitance in regard to the discharge waveform.

The Charging Circuit

Alternator Terminal Measurements of Voltage and Current. Various measurements were made at both primary and secondary points for the circuit of Figure 8. The current and voltage waveforms at the alternator terminals were needed to help determine the impact of resonant loading on the power source. The oscillogram of Figure 12 shows the primary current and voltage at the alternator terminals with the system operating at a speed of 2250 RPM (450 Hz) and excited to an output power level of 45 KW. All system measurements were taken with a constant DC voltage applied to the exciter field since a satisfactory voltage regulator was not available for this function.

Though some differences may be noted, the general appearance of the waveforms is sinusoidal. This was, in particular, expected for the voltage waveform. It contains a number of abrupt changes which are due to the turning on of the diodes in the pulser. Note that there are six transients per cycle. This number corresponds to the number of diodes. The two largest transients occur near the C phase voltage zero crossing and reflect the turn on of the two diodes in this particular phase. Any

time a diode in one phase turns on it disturbs the resultant armature reaction flux and, thus, the resultant air gap flux. This disturbance affects all phases, especially the phase containing the diode that turned on. One other point to be noted is that the voltage does not experience any sagging as the current rises to a peak. This was one of the problems reported by Lt Silva in his investigation of DC resonant charging (Ref 8: 32-36).

The current waveform in Figure 12 presents the typical tsint shape. Recall from equation (4) that the theory predicted this type of waveform. Though not pictured, the waveforms for 15, 30, and 60 KW had the same general appearance as those shown in Figure 12.

Pulser Measurements. Figure 13 shows the charging current and voltage waveforms for one of the two charging circuits of Figure 4. The measurements were made at a point between the diode and the 0-5 amp ammeter. The machine was delivering approximately 20 KW at 2200 RPM (440 Hz). As in Figure 12, the half cycle charging current waveform displays the basic tsint shape. The general form of this curve compares favorably with the calculated charging current curve in Figure 9. However, these curves cannot be compared on a magnitude basis since a value for the driving voltage is assumed in Figure 9 but is unknown (and cannot very easily be determined) for the oscillogram.

The charging voltage waveshape in the oscillogram closely resembles the VC curve in Figure 10. However, the calculated voltage values in Figure 10 have been referred to the transformer primary. This, plus the problem concerning the unknown internal emf, means that the two voltage waveforms cannot be compared on a quantitative basis.

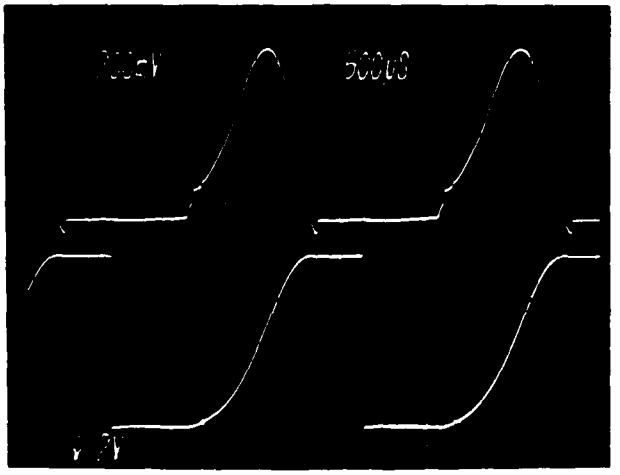

Figure 13. Charging Current and Voltage

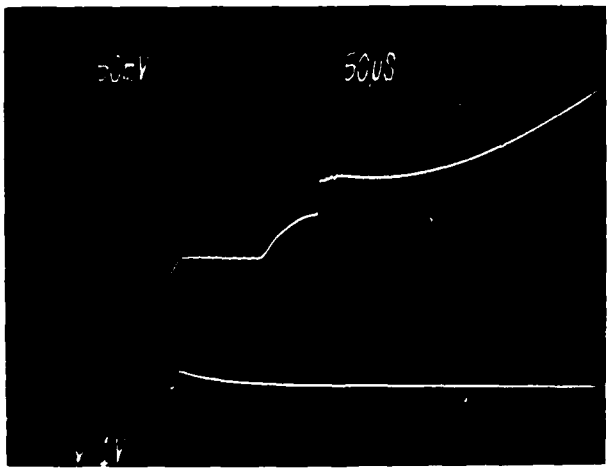

Figure 14. Initial Rise of the Charging Current

The charging voltage and current waveshapes for various frequencies and power levels present a number of unexpected deviations. These anomalies will now be discussed.

Charging Current Anomalies. One of the irregularities associated with the charging current waveform occurs at the end of the half cycle. Figure 13 shows that the current passes through zero and briefly stays negative. A close examination of the charging voltage reveals that it decreases slightly at this same time. This implies that the current reverses direction and reduces the charge on the capacitor by a minute amount. These actions are possible only because the hold-off diode is a combination of resistors, capacitors, and diodes; that is, it is a stacked rectifier. Its components are listed in Appendix D. While the charging current is positive the compensating capacitors in the rectifier are fully charged in one direction. As the source (high voltage transformer terminals) begins to change its polarity the large voltage on the charging capacitor forces an immediate voltage reversal on the compensating capacitors. This also causes the circuit current to briefly go negative. This current removes charge from the storage capacitor to the compensating capacitors which, when fully charged, reduce the current back to zero. The amount of charge involved in this transfer is so small that it is barely detectable on the voltage oscillogram.

The charging current waveform also has an irregularity at the beginning of the half cycle. The initial rise in the charging current of Figure 13 is shown in Figure 14. Again, the hold-off diode is believed to be responsible for this deviation. The vertical transient of approximately 0.3 amps is difficult to explain since the charging circuit contains such a large charging inductance. This inductance of

approximately 0.3 henries (referred to the secondary) should eliminate any high di/dt component. The rounded portion of the initial current rise seems to be caused by the resonating effect of the charging inductance with the compensating capacitors in the rectifier stack. These components produce a response which reaches a peak in approximately 35.7 μsec. Though this value is quite different from the 50 μsec oscillogram time, it seems to be a reasonable method for analyzing the current initiation.

Charging Voltage Anomaly. The charging voltage curve in Figure 13 looks almost like the ideal textbook curve. However, the initial tests resulted in the curve shown in Figure 15. The charging voltage begins at zero or some negative value. After a brief rise it suddenly experiences a transient. A blowup of a similar transient observed in a later test is shown in Figure 16.

There are two major reasons for the difference in the voltage curves of Figures 13 and 15. The alternator speed and thyratron hold-off inductance for the transient-plagued curve of Figure 15 were 2000 RPM and 51 μh, respectively. The smooth curve of Figure 13 was obtained at a speed of 2200 RPM and the inductance was reduced to 29 μh. The reduction in the inductance was primarily made in order to lower the reverse voltage on the charging capacitor at the end of each discharge. A reduction in the charging voltage transient turned out to be a positive side effect of this change. Though not as evident, the transient reappeared at higher power levels. Thus, the changes in frequency and inductance helped but did not eliminate the source of the problem.

Since the magnitude of the transient depended upon the value of the thyratron turn-off inductance, the possibility of an interaction between

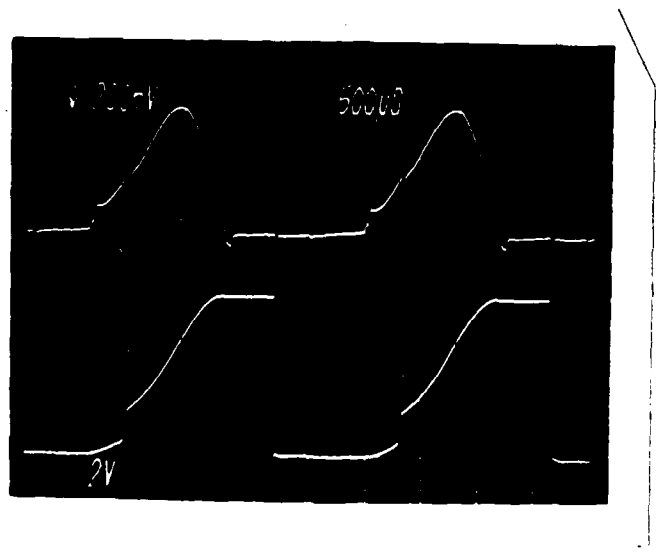

Figure 15. Initial Charging Voltage Curve with Transient

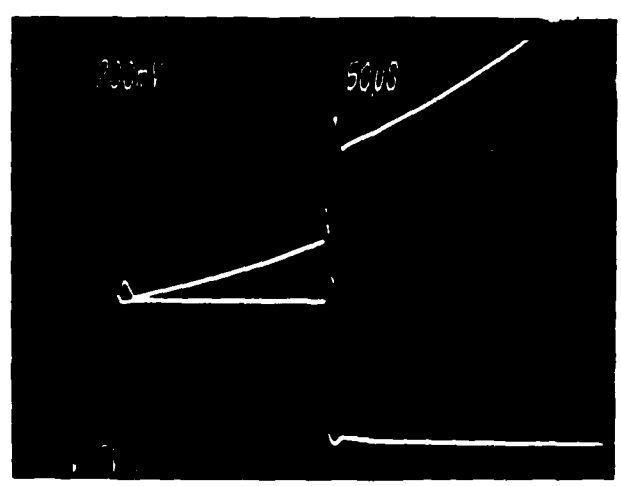

Figure 16. Blowup of Charging Voltage Curve Transient

the charge and discharge circuits of the phase was investigated. The charging voltage curve for one circuit of the phase was observed after disconnecting the external trigger input to the thyratron grid in the second circuit. This effectively removed the second circuit from the phase. When this was done the transient was eliminated.

Thus, it appears that the problem stems from voltage spikes produced by the thyratron turn-off inductance in each discharge circuit. In order to analyze the interaction between the circuits the schematic diagram of the pulser has been simplified as shown in Figure 17. The circuit analysis may begin by assuming that C1 has been fully charged and is awaiting discharge through thyratron T1. The charging of C4 has just begun. Thus, CR1 is turned off and CR4 is turned on. If T1 is now triggered to close,

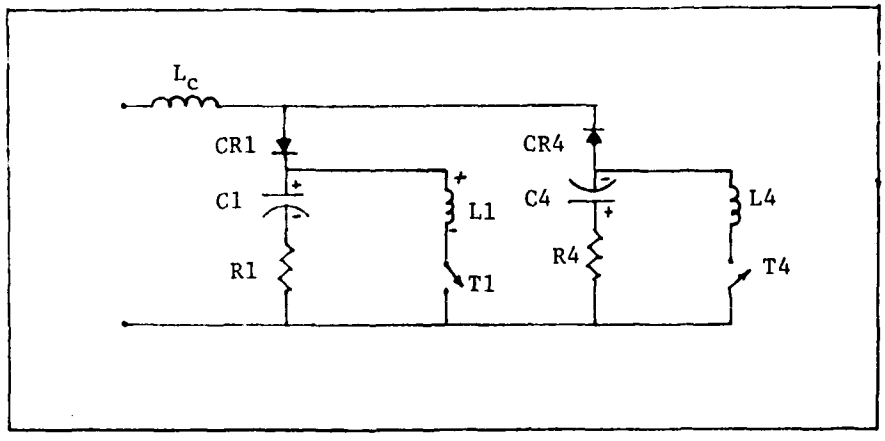

Figure 17. Simplified Pulser Schematic for Studying the Charge/Discharge Interaction

the discharge current through it causes the voltage on L_1 (V_{L1}) to go positive and then negative. As the current approaches zero this reversed polarity voltage reaches a magnitude that exceeds the slow

rising voltage on capacitor C4. (It also exceeds the source voltage. However, the charging inductance, LC, completely isolates the source from this transient.) When the voltage on C4 is exceeded, CR1 turns on. The charge which would have gone into building up additional reverse bias on C1 is now shunted onto C4. The current path for this charge is L1, T1, R4, C4, CR4, and CR1. When the discharge current passes through zero, switch T1 opens, V_{L1} drops back to zero, and the transient ends.

From the transient standpoint it would be sufficient to remove L1 and L4 from the circuit. However, they are required in order to assure the turn-off of the thyratrons. Thus, for this particular pulser the symptom, rather than the cause, must be addressed. One approach is to incorporate an SCR in series with each rectifier stack. The trigger timing should allow the SCR to turn on only during the charging half cycle. Therefore, even if the transient should forward bias the SCR, it will not turn on and, thus, the voltage spike due to L1 will have no effect on the C4 charging branch. This method does, unfortunately, make additional requirements for hardware and triggering.

Readjustment of the thyratron trigger control box settings is another approach that may be taken to resolve the voltage transient problem. The firing mechanism should allow the voltage on the storage capacitor (C4) to exceed the inductor voltage spike at the time of discharge. This means that capacitor C1 must be discharged at a later time during the half cycle. Thus, the new settings should prevent the turn-on of the diode in the discharge branch since it will always be reverse biased. The settings presently initiate the discharge when the source voltage reaches a particular amplitude during the negative half cycle.

Many questions were left unanswered concerning the voltage and current waveform anomalies. They were investigated primarily to gain a qualitative understanding of their underlying causes. However, any further examination was considered to be beyond the scope of this study.

Resonance Determination

Including all of the system charging inductance in the alternator could possibly reduce the power source weight by as much as 1/3 (Ref 6). This would remove the necessity for the high leakage transformer which was used in the MERADCOM charging circuit. In an operational system a pulse transformer between the PFN and load could provide any additional voltage multiplication needed for the discharge pulse. Before the transformer leakage inductance can be incorporated into the alternator its internal inductance for the AC resonant mode should be determined. It is the combination of these two inductances that must then be designed into the high reactance machine. However, determining the internal inductance, L_a, turns out to be a difficult task.

There is a tendency to use classical steady state theory for determining L_a. The initial step is to find the resonant frequency, ω_o. The inductive and capacitive reactances should be equal at this frequency. Thus,

$$X_L = X_C \tag{7}$$

or

$$L_c = 1/(\omega_o{}^2 C_N) \tag{8}$$

where

L_c = total charging inductance

C_N = network charging capacitance

Since L_c consists of the internal alternator inductance plus the transformer leakage inductance, L_x, then L_a may be written as

$$L_a = L_c - L_x \tag{9}$$

The difficulty with the above approach is that classical steady state resonant theory is not applicable. A popular circuit analysis text states, "Resonance, by definition, is fundamentally associated with the forced response since it is defined in terms of a purely resistive input impedance, a sinusoidal steady state concept" (Ref 3:450). The response of the MERADCOM system for half cycle charging includes both a forced and a transient component. This is evident from the exponential terms in equations (2) and (3). Thus, the system never reaches steady state in the classical sense. This means that the system input impedance never becomes purely resistive. At the beginning of each half cycle the source "sees" the same input, a large inductor in series with a capacitor charged to a slightly negative value. If the blocking diode of Figure 7 was removed, a number of half cycles of charging would be required to get the system past the transient state. Only then would the impedance be resistive and the output waveforms sinusoidal. With the present system configuration only the input is sinusoidal and even it is slightly deformed by the turn-on of the diodes. Therefore, since the source never "sees" past the first half cycle, it continuously faces a circuit which contains some reactance and has a transient response. Thus, equation (7) is never realized.

In most resonant circuits a number of parameters can be varied until resonance is detected. For example, changing either L, C, or the frequency f should yield the circuit response needed to obtain resonance. However, the frequency is usually chosen as the variable parameter. Regardless of the selected variable, the source terminal voltage is maintained constant. This provides the standard from which measurements can be evaluated. For example, resonance in the typical series RLC circuit, as shown in Figure 7 with the diode removed, is obtained by holding the source terminal voltage (point B) constant and varying f until a peak current is reached. This occurs when the circuit becomes purely resistive, that is, when the inductive and capacitive reactances cancel as expressed in equation (7). When this happens a power factor of unity may be measured at the source terminals and the current will be in phase with the terminal voltage.

The nature of this research effort removes the constant terminal voltage standard since part of the charging inductance is inside the alternator. It is now desired to hold the voltage at point A of Figure 7 constant and vary f until the peak current is reached. Also, this current should be in phase with the voltage at point A. L_a is assumed to be approximately constant and C is fixed. The difficulty with this procedure is that E_a, the internally generated emf under load, is inaccessible. If it could be measured it would be a simple task to keep it constant by varying the excitation.

The exciter circuit for the charging system is shown in Figure 8. The circuit enclosed in the dashed block rotates at the same speed as the rotor. It produces a flux which is then conditioned by the armature reaction. The resulting flux then induces the alternator voltage E_a which is approximated in the following equation.

$$E_a = 4kN\phi f \qquad (10)$$

where

k = form factor to account for non-sinusoidal aspects

N = number of turns linked by the flux

ϕ = peak amplitude of the resultant flux

f = impressed frequency in Hz

Although equation (10) shows that E_a is a function of ϕ and f it does not infer that ϕ is itself a function of f. This is the case, however, since an increase in f leads to an increase in the alternator field current for constant exciter current. The field flux is then boosted due to this larger current. Thus, the total change in E_a results not only from the increase in frequency but also from the variation in flux due to the frequency change.

From the previous discussion it appears that there is no direct method for determining resonance and, hence, L_a. Thus, an indirect approach was taken which may be used to approximate L_a.

At unity power factor (behind the machine inductance) E_a should not be much greater than the terminal voltage V_T and can be calculated if a value for L_a is assumed. Since E_a cannot be measured, this one value is of little help. However, if E_a is calculated for a number of frequencies and is then divided by the measured current I_a for these same frequencies, an impedance trend (Z versus f) is developed. This procedure was followed for a number of values for L_a. The goal was not to determine the frequency at which the impedance became purely resistive but rather the frequency at which it became a minimum. As indicated earlier, the circuit is in a transient mode and its input impedance will always be somewhat reactive. The equation used to calculate E_a was

$$E_a\underline{/\phi} = V_T\underline{/0°} + I_a\underline{/\theta}\ (R_a + j\omega_a L_a) \qquad (11)$$

where

E_a = internally generated emf (volts rms)

V_T = alternator terminal voltage (volts rms)

I_a = phase current measured at the alternator terminal (amps rms)

ϕ = angle between V_T and E_a (degrees)

θ = angle between V_T and I_a (degrees)

R_a = 0.27 = internal phase resistance of the alternator (ohms)

ω_a = alternator frequency (radians/second)

L_a = selected alternator internal inductance (henries)

The various parameters and values which were associated with equation (11) are listed in Table I. All measurements were taken with the generator field current held to a constant value of 8.0 amps. A number of values for L_a were selected and evaluated. However, only three are listed in the table. The first value selected was 0.218 mh, the specification sheet leakage inductance. As the frequency was varied the impedance Z reached a minimum at 2275 RPM. Although this may indeed be the frequency at which the minimum impedance occurs it is also the frequency at which the system started to become slightly unstable. It is believed that the 60 KW tests caused some problems in the switching circuits. There was insufficient time to try to correct this problem and, thus, some instability was noticed at the higher speeds.

As noted above, the choice of 0.218 mh for L_a resulted in a minimum impedance at 2275 RPM or 2859 rad/sec. This frequency can now be substituted into equation (12) to determine the validity of the L_a selection.

$$\omega_a = \left[\frac{1}{L_c C_N} - \left(\frac{R_c}{2L_c}\right)^2\right]^{1/2} \qquad (12)$$

Table I

Data Used to Study the Alternator Response and Its Internal Reactance

RPM	θ(DEG)	I_a	V_T	E_f	L_a = 0.3E-3		L_a = 0.218E-3		L_a = 0.165E-3	
					E_a/ϕ	$Z/\phi-\theta$	E_a/ϕ	$Z/\phi-\theta$	E_a/ϕ	$Z/\phi-\theta$
1800	24.0	33.2	134	177	135/10	4.07/-14	137/8	4.12/-16	138/6	4.16/-18
1900	23.3	34.4	137	188	138/11	4.02/-12	140/8	4.07/-15	141/7	4.1/-17
2000	19.4	40.3	144	196	147/13	3.65/-7	148/9	3.68/-10	150/7	3.71/-12
2100	12.1	41.8	135	206	143/14.0	3.43/1.9	143/10	3.43/-2	144/8	3.44/-4
2125	12.2	43.0	137	208	146/14.3	3.39/2.1	146/11	3.38/-1.6	146/8.2	3.39/-4
2150	11.0	43.0	136	211	145/14.5	3.38/3.5	145/10.8	3.37/-0.2	145/8.3	3.38/-2.7
2175	10.3	43.0	136	213	146/14.6	3.39/4.3	145/10.8	3.38/0.5	145/8.4	3.38/-2
2200	9.5	43.2	135	216	146/14.9	3.36/5.4	145/11.0	3.35/1.5	145/8.5	3.35/-1
2225	9.3	43.4	134	218	145/15.1	3.34/5.8	144/11.2	3.32/1.9	144/8.6	3.32/-0.7
2250	9.6	43.8	132	221	143/15.7	3.26/6.1	142/11.6	3.25/2.0	142/8.9	3.25/-0.6
2275	9.7	42.0	123	221	133/16.3	3.17/6.7	132/12.1	3.15/2.4	132/9.3	3.15/-0.3
2300	9.8	40.8	120	223	130/16.4	3.19/6.6	129/12.1	3.17/2.4	129/9.3	3.17/-0.4
2325	9.9	41.1	125	225	135/16.1	3.27/6.2	134/11.9	3.26/2.1	134/9.2	3.42/-0.7
2350	10.0	40.2	129	229	138/15.5	3.43/5.5	137/11.5	3.42/1.5	137/8.8	3.42/-1.1

where

R_c = 0.445 = total charging circuit resistance (ohms) and the remaining terms have been previously defined. This equation, when solved for L_c, yields

$$L_c = \frac{1}{2\omega_a^2 C_N} \pm \frac{1}{2}\left[\left(\frac{1}{\omega_a^2 C_N}\right)^2 - \left(\frac{R_c}{\omega_a}\right)^2\right]^{1/2} \qquad (13)$$

Upon substituting ω_a = 2859 rad/sec, C_N = 142 μf, and R_c = 0.445 ohms into equation (13), L_c is found to be 0.855 mh. Subtracting the transformer inductance of 0.69 mh from this gives a value for L_a of 0.165 mh.

This value may now replace the initially selected value of 0.218 mh for L_a. With this new value E_a and Z are calculated for varying frequencies. As Table I shows, the minimum Z (both magnitude and angle) occurs at 2275 RPM. (The calculated angle cannot be viewed quantitatively.) This same speed resulted for each selection of L_a. Thus, the alternator supplies an internal inductance of approximately 0.165 mh at a resonant frequency of 455 Hz. However, the data in the last column of Table I implies that the "resonant bandwidth" may be quite wide. Since the alternator waveforms are similar to sinusoids, the bandwidth, as with steady state theory, should depend upon the Q of the circuit. This factor is relatively low (approximately 5) and, therefore, supports the conclusion of a wide bandwidth.

The value of X_a, determined from L_a, may now be compared with the values of reactance found in the alternator specifications sheet. For this comparison it is transformed into its per unit reactance value. This is accomplished by the following equation

$$X_a = 2\pi f L_a/(V_B/I_B) \text{ per unit (pu)} \qquad (14)$$

where

f = 400 = design frequency (Hz)

V_B = 240 = base voltage (volts)

I_B = 26 = base current (amps)

Substituting these values and L_a = 0.165 mh into equation (14) gives a value of 0.0449 pu for X_a. The only reactance value in the specification sheets that is in this magnitude range is the armature leakage reactance. Its value is 0.0594 per unit. Thus, the value for X_a appears to be slightly lower than the leakage reactance value.

The alternator should respond differently for a transient condition and a steady state operation unless the transient is of such a nature that it is viewed by the machine as steady state. As explained earlier, half cycle charging produces a transient response. So now the point of interest is how this particular transient response impacts the operation of the alternator. A second use of the measured data in Table I may be made in order to investigate this point. The data will be applied to the two-reaction method for computing the angle ψ between the phase current I_a and the open circuit voltage E_f (Ref 1:114; 7:204-212). The steady state reactance components will be used in conjunction with this data in order to develop the vector diagram drawn in Figure 18. The two-reaction method assumes steady state operation. Thus, if the approach is still applicable using the measured data then it strongly suggests that the alternator views the system operation as steady state (nearly sinusoidal). The following equations will also be useful in this development.

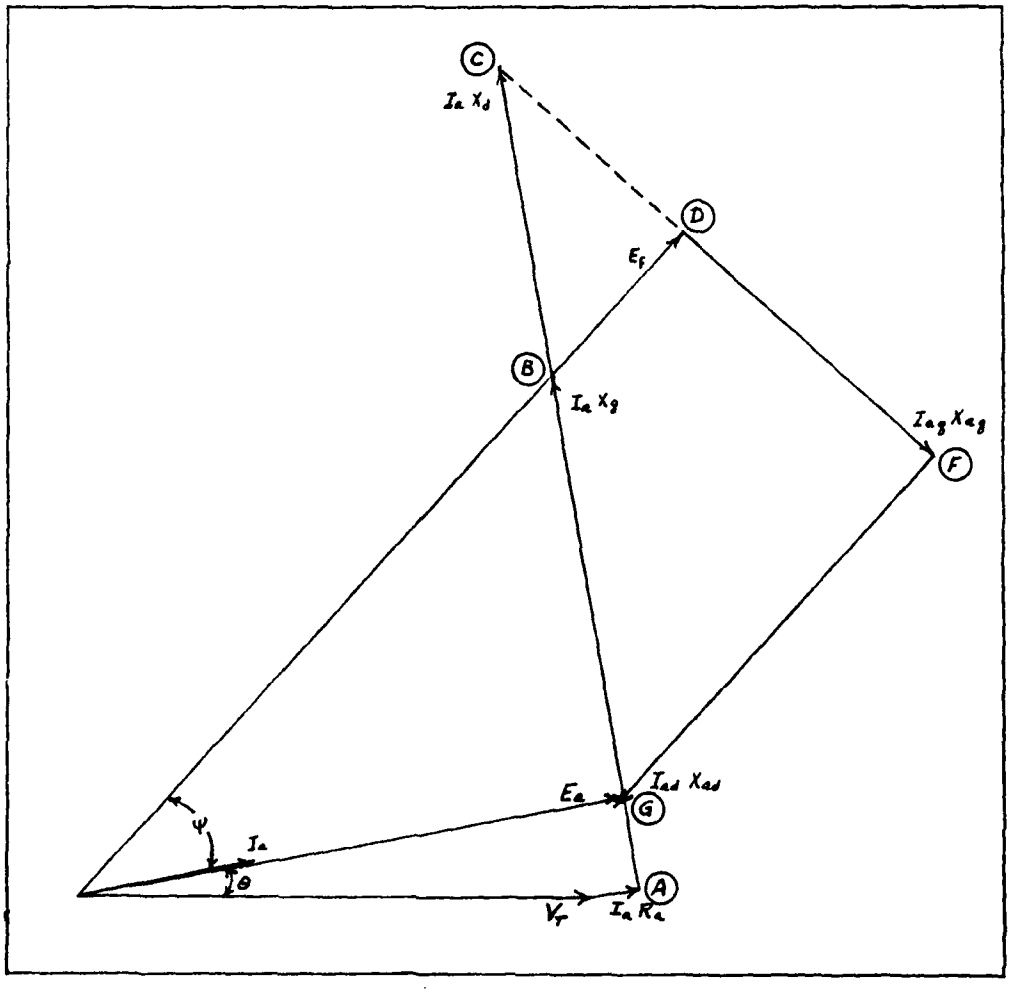

Figure 18. Alternator Vector Diagram Using Steady State Reactance Components (2275 RPM)

$$I_{ad} = I_a \sin\psi \tag{15}$$

$$I_{aq} = I_a \cos\psi \tag{16}$$

$$X_{ad} = X_d - X_\ell \tag{17}$$

$$X_{aq} = X_q - X_\ell \tag{18}$$

where

I_a = phase current (amps)

ψ = angle between E_f and I_a (degrees)

I_{ad} = direct component of the phase current (amps)

I_{aq} = quadrature component of the phase current (amps)

X_ℓ = leakage reactance (ohms)

X_d = direct axis synchronous reactance (ohms)

X_{ad} = direct component of reactance (ohms)

X_q = quadrature axis synchronous reactance (ohms)

X_{aq} = quadrature (or cross) component of reactance (ohms)

The terminal voltage V_T is first drawn along the horizontal. I_a is then drawn at an angle θ and the I_aR_a drop is laid off parallel to I_a. R_a is the internal resistance of the alternator and was measured to be approximately 0.27 ohms. From point A the line AC is drawn perpendicular to I_a with the magnitude I_aX_d. AB is laid off along this same line by the amount I_aX_q. The angle between E_f and I_a, ψ, is now found by extending a line from the origin through B. The magnitude of E_f is determined by segment CD which is drawn perpendicular to this line. This value should closely approximate the measured open circuit voltage if the alternator may be viewed as operating in a steady state mode.

The direct and quadrature components of the phase current may now

be used to find the internally generated voltage, E_a. This is begun by first extending a line from point D to point F. It is parallel to CD and has a magnitude $I_{aq}X_{aq}$. The vector $I_{ad}X_{ad}$ is then drawn perpendicular to this line. It begins at point F and should terminate at some point G on line segment AB. The vector for the internally generated voltage E_a may then be drawn from the origin to G. The final vector of interest connects points A and G and should have a value I_aX_ℓ.

Many system transients are of such a nature that they induce transient currents inside the alternator. For this case the synchronous reactance values cannot be used in the development of the vector diagram in Figure 18. A use of these values would cause the diagram to be in error. Most notable, E_f would be incorrect in magnitude and direction and, hence, would not equal its measured value.

Under certain circumstances the operation of the alternator may be viewed as steady state even though it feeds a circuit experiencing a transient response. Apparently, this is what is happening during AC resonant charging and, thus, the use of the synchronous reactances in the development of the alternator vector diagram is permissible.

There are a number of reasons the alternator may be considered to be operating in the steady state. At the beginning of each charging half cycle the circuit connected to the alternator terminals is changed. Just before this half cycle begins the source is completing the build-up of peak charge on one capacitor. At the completion of this build-up the charged capacitor circuit is replaced with a circuit containing a capacitor holding a slightly negative charge. This new circuit results in a mathematically transient response (see equation (2)). However, the response is so gradual (primarily due to the large charging inductance)

that the alternator can barely distinguish it from 400+ Hz operation. As shown in Figure 12, it contains no current discontinuities at the half cycle end points or during the charging of the capacitor. The smooth transition at the end points is primarily due to the initial condition requirements. These are specified in Appendix A which shows that the current must be zero at both the beginning and end of a half cycle. All of these characteristics combine to produce a repetitive waveform at the alternator terminals and an armature reaction that is fixed both in magnitude and direction with respect to the poles. The fixed nature of the armature reaction prevents the build-up of the voltages which cause transient currents inside the machine (Ref 5:286-290). Thus, synchronous reactances may be used in developing a two-reaction alternator vector diagram as shown in Figure 18. The vectors drawn in this diagram were based upon Table I measurements taken at 2275 RPM and the synchronous alternator reactances listed in Appendix D. The diagram results in an open circuit voltage of 215 volts. The terminal point of the $I_{ad}X_{ad}$ vector is slightly past line AB. The distance from this point to A is measured to be approximately 24.6 volts which results in a value for X_{ℓ} of 0.064 per unit. This per unit value is just slightly larger than the 0.0594 leakage reactance value specified for the alternator. Similarly, the graphical value of E_f is 6 volts less than the measured value of 221 volts. These differences are well within the realm of error in measurement. The results indicate that although half cycle charging is a transitory condition it allows the alternator to experience a mode of operation that very closely resembles steady state.

IV. Conclusions and Recommendations

There were a number of objectives associated with this study. One of the most important was to determine the impact on an alternator when it operates in the AC resonant charging mode. Its output waveforms were to be analyzed for degradation while varying the load and frequency. The final objective was to determine, if possible, when the system was at resonance. This was equivalent to determining the internal reactance of the machine.

Conclusions

The system was successfully tested for 15, 30, and 45 KW. However, only a few measurements were taken at the 60 KW level due to the development of trigger circuit problems. These load variations did not cause any noticeable degradation of the alternator operation. A similar conclusion was reached when the frequency was varied from approximately 380 to 475 hertz. This, to some extent, results from a low circuit Q of approximately 5.

Although a number of anomalies were detected in the charging waveforms, the waveshapes very closely conformed to the theoretical predictions. The anomalies were found to be peculiar to the hardware and configuration of the system under investigation.

During the latter tests, system noise tended to aggravate the trigger circuits and caused pre-firing of certain thyratrons that must have been adversely affected during the 60 KW tests. Reducing the gas pressure inside the thyratron tubes could have possibly alleviated this condition.

No straightforward method was developed for determining precise resonance. The term resonance as used in this study context is somewhat of a misnomer since classical steady state resonant theory is not really applicable. Classical theory addresses only the forced response. This study showed that the transient response cannot be excluded. Classical theory also seeks a maximum amplitude response when all reactances cancel and the system is purely resistive. This study concludes that the half cycle charging circuit has a transient response. The reactances do not completely cancel and, thus, the input impedance is never purely resistive. Even so, the alternator armature reaction is approximately fixed, both in magnitude and direction, with respect to the poles. This implies that the alternator is in a near steady state mode of operation. This latter point was confirmed by the use of measured data and synchronous reactances in a two-reaction vector analysis for the alternator. This same data was used to determine the internal reactance of the alternator during resonant charging. It was found to be slightly less than the armature leakage reactance.

Recommendations

The literature search for this study led to the conclusion that there is only scant material on charging systems. Thus, an investigation of methods other than AC or DC resonant charging would contribute to filling this void. One method, in particular, which has caught the interest of the Army (MERADCOM) is network charging. This method limits the peak current requirements and is not expected to cause as negative an impact on the alternator as does DC resonant charging. Further, its controls and triggering should be simpler than those needed for AC resonant charging. It needs to be investigated and compared with the methods already studied.

The AC pulser is a very basic prototype. The MERADCOM engineers were aware of many of its shortcomings before its delivery. If these design problems could be corrected this would permit more reliable and expanded testing. In addition to redesigning the trigger controls, consideration would have to be given to wiring, grounding, noise suppression, and the general physical layout of the circuit.

Bibliography

1. Bailey, Benjamin F. and James S. Gault. Alternating-Current Machinery. New York, Toronto, and London: McGraw-Hill Book Company, 1951.

2. Glasoe, G. N. and J. V. LeBacqz. Pulse Generators. New York and London: McGraw-Hill Book Company, 1948.

3. Hayt, William H., Jr. and Jack E. Kemmerly. Engineering Circuit Analysis. New York, San Francisco, Toronto, and London: McGraw-Hill Book Company, 1962.

4. Kuhlmann, John H. Design of Electrical Apparatus (Third Edition). New York: John Wiley and Sons, 1950.

5. Lawrence, Ralph R. and Henry E. Richards. Principles of Alternating-Current Machinery (Fourth Edition). New York, Toronto, and London: McGraw-Hill Book Company, 1953.

6. O'Loughlin, James P. Electrical Engineer, Air Force Weapons Laboratory (personal interview). Kirtland AFB, New Mexico, June 16, 1981.

7. Puchstein, A. F., T. C. Lloyd, and A. G. Conrad. Alternating-Current Machines (Third Edition). New York: John Wiley and Sons; London: Chapman and Hall, Limited, 1958.

8. Silva, Jaime R. "Prime Power to Pulse Conditioning Interface Methods." MS Thesis. School of Engineering, Air Force Institute of Technology, Wright-Patterson AFB, Ohio, December 1980.

9. 75-11605, Addendum 2. "Subsystem Design Analysis, Lightweight Alternator (Model Test Program)." Preliminary Final Report prepared for the Air Force Special Weapons Center, Kirtland AFB, New Mexico. Torrance, California, Airesearch Manufacturing Company of California, June 30, 1976.

Appendix A

Theoretical Development of the AC Resonant Charging Equations

The following analysis is taken from Ref 2. The differential equation for the circuit of Figure 7, in terms of the network charge q_N, is

$$L_c \frac{d^2 q_N}{dt^2} + R_c \frac{dq_N}{dt} + \frac{1}{C_N} q_N = E_a \cos(\omega_a t + \phi) \qquad \text{(A-1)}$$

The steady state solution of equation (A-1) has the form

$$q_1(t) = \bar{Q}_N \, \varepsilon^{j\omega_a t} \text{ coulombs} \qquad \text{(A-2)}$$

where $\bar{Q}_N$ is found by substituting (A-2) into (A-1). Thus,

$$\bar{Q}_N = \frac{C_N E_a \varepsilon^{j\phi}}{1 - L_c C_N \omega_a^2 + j R_c C_N \omega_a} \text{ coulombs} \qquad \text{(A-3)}$$

The transient integral for (A-1) is

$$q_2(t) = \bar{A} \, \varepsilon^{\bar{p}t} \text{ coulombs} \qquad \text{(A-4)}$$

where

$\bar{A}$ is a complex constant of integration

$$\bar{p} = -a + j\omega = -\frac{R_c}{2L_c} + j\sqrt{\frac{1}{L_c C_N} - \left(\frac{R_c}{2L_c}\right)^2} \qquad \text{(A-5)}$$

The complete solution for (A-1) is then

$$q_N(t) = q_1(t) + q_2(t) = \bar{Q}_N \, \varepsilon^{j\omega_a t} + \bar{A} \, \varepsilon^{\bar{p}t} \qquad \text{(A-6)}$$

For the general case the following initial conditions at t = 0 may be assumed

$$q_N(t) = q_N(0)$$

$$i_c(t) = i_c(0)$$

Substituting these values into equation (A-6) and the time derivative of (A-6) gives

$$q_N(0) = \mathrm{Re}(\bar{Q}_N + \bar{A}) = Q_1 + A_1$$

$$i_c(0) = \mathrm{Re}(j\omega_a \bar{Q}_N + \bar{p}\bar{A}) = -\omega_a Q_2 - aA_1 - \omega A_2$$

Solving for A_1 and A_2,

$$A_1 = q_N(0) - Q_1 \tag{A-7}$$

$$A_2 = -\frac{1}{\omega}\{i_c(0) + \omega_a Q_2 + a[q_N(0) - Q_1]\} \tag{A-8}$$

where the abbreviation "Re" means "real part of".

Now let

$$A = |\bar{A}| = |A_1 + jA_2|$$

ψ = phase angle of $\bar{A} = \arctan \dfrac{A_2}{A_1}$

$$Q_N = |\bar{Q}_N| = |Q_1 + jQ_2|$$

θ = phase angle of circuit = $\arctan \dfrac{R_c C_N \omega_a}{1 - L_c C_N \omega_a^2}$

Thus, equation (A-3) may be written as

$$\bar{Q}_N = Q_N \, \varepsilon^{j(\phi - \theta)} \tag{A-9}$$

The solution for $q_N(t)$ may then be written

$$q_N(t) = \mathrm{Re}(\bar{Q}_N \, \varepsilon^{j\omega_a t} + \bar{A} \, \varepsilon^{\bar{p}t})$$

$$q_N(t) = Q_N \cos(\omega_a t + \phi - \theta) + A \, \varepsilon^{-at} \cos(\omega t + \psi) \tag{A-10}$$

Now, differentiating (A-10)

$$i_c(t) = \omega_a Q_N \{-\sin(\omega_a t + \phi - \theta)\} + A\{-\varepsilon^{-at} \omega \sin(\omega t + \psi) - a \, \varepsilon^{-at} \cos(\omega t + \psi)\}$$

or

$$i_c(t) = \omega_a Q_N \cos(\omega_a t + \phi - \theta + \frac{\pi}{2}) + \omega_o A \varepsilon^{-at} \cos(\omega t + \psi + \beta) \tag{A-11}$$

where

$$Q_N = \left| \frac{C_N \, E_a}{1 - L_c C_N \omega_a{}^2 + j R_c C_N \omega_a} \right| = \left| Q_1 + j Q_2 \right|$$

ω = angular frequency of circuit

$\beta = \arctan \frac{\omega}{-a}$

$\omega_o = \sqrt{\omega^2 + a^2}$

For AC resonant charging the circuit frequency, ω, is set equal to the impressed frequency, ω_a. With $\omega = \omega_a$ equation (A-10) becomes

$$q_N(t) = Q_N\cos(\omega_a t + \phi - \theta) + A\,\varepsilon^{-at}\cos(\omega_a t + \psi) \qquad \text{(A-12)}$$

Expanding $\cos(\omega_a t + \psi)$ and recognizing that $A_1 = A\cos\psi$ and $A_2 = A\sin\psi$ (A-12) becomes

$$q_N(t) = Q_N\sin(\omega_a t + \phi) + \varepsilon^{-at}[A_1\cos\omega_a t - A_2\sin\omega_a t]$$

A_1 and A_2 in this equation can now be replaced with the right side of equations (A-7) and (A-8). Making these changes and substituting $Q_N\sin\phi$ for Q_1 and $Q_N\cos\phi$ for Q_2 yields the equation for the network charge

$$q_N(t) = Q_N(1 - \varepsilon^{-at})\sin(\omega_a t + \phi) + \varepsilon^{-at}\{q_N(0)\cos\omega_a t + \left(\frac{i_c(0)}{\omega_a} + \frac{aq_N(0)}{\omega_a} - \frac{a}{\omega_a}Q_N\sin\phi\right)\sin\omega_a t\} \qquad \text{(A-13)}$$

The condition for repeating transients is, for half cycle charging, $i_c(\pi) + i_c(0) = 0$. The current is now obtained by differentiating equation (A-13) and is

$$i_c(t) = \frac{E_a}{R_c}(1 - \varepsilon^{-at})\cos(\omega_a t + \phi) + \varepsilon^{-at}\{i_c(0)\cos\omega_a t - \omega_a q_N(0)\sin\omega_a t + \frac{E_a}{2L_c\omega_a}\sin\omega_a t\cos\phi\} + \frac{a}{\omega_a}\varepsilon^{-at}\{\frac{E_a}{2L_c\omega_a}\sin\phi - i_c(0) - aq_N(0)\}\sin\omega_a t \qquad \text{(A-14)}$$

where $\frac{E_a}{R_c\omega_a}$ has been substituted for Q_N.

At $\omega_a t = \pi$ equation (A-14) becomes

$$i_c(\pi) = -\frac{E_a}{R_c}(1 - \varepsilon^{-\frac{\pi a}{\omega_a}})\cos\phi - \varepsilon^{-\frac{\pi a}{\omega_a}} i_c(0) = -i_c(0)$$

Solving for $i_c(0)$ yields

$$i_c(0) = \frac{E_a}{R_c}\cos\phi \tag{A-15}$$

The quality factor Q is defined as

$$Q = \frac{L_c\omega_a}{R_c} = \frac{1}{R_c C_N \omega_a} \tag{A-16}$$

By substituting $i_c(0)$ and Q into (A-13) a revised equation for the network charge is obtained

$$q_N(t) = Q\,C_N E_a\,(1 - \varepsilon^{-\frac{\omega_a t}{2Q}})\sin(\omega_a t + \phi) + \varepsilon^{-\frac{\omega_a t}{2Q}}\{q_N(0)\cos\omega_a t + (QC_N E_a\cos\phi - \frac{C_N E_a}{2}\sin\phi + \frac{1}{2Q}q_N(0))\sin\omega_a t\} \tag{A-17}$$

This equation is then differentiated to produce the charging current,

$$i_c(t) = QC_N E_a\omega_a\,(1 - \varepsilon^{-\frac{\omega_a t}{2Q}})\cos(\omega_a t + \phi) + \varepsilon^{-\frac{\omega_a t}{2Q}}\{QC_N E_a\omega_a\cos\phi\cos\omega_a t - [C_N E_a\omega_a(\frac{q_N(0)}{C_N E_a} - \frac{1}{4Q}\sin\phi) - \frac{q_N(0)\omega_a}{4Q^2}]\sin\omega_a t\} \tag{A-18}$$

This expression may then be restructured to give

$$i_c(t) = QC_N E_a \omega_a \{(1 - \varepsilon^{-\frac{\omega_a t}{2Q}})\cos(\omega_a t + \phi) + \varepsilon^{-\frac{\omega_a t}{2Q}}[\cos\phi\cos\omega_a t$$

$$- (\frac{q_N(0)}{QC_N E_a}(1 - \frac{1}{4Q^2}) - \frac{1}{4Q^2}\sin\phi)\sin\omega_a t]\} \qquad \text{(A-19)}$$

which, for most values of Q, can be approximated by

$$i_c(t) = QC_N E_a \omega_a \{(1 - \varepsilon^{-\frac{\omega_a t}{2Q}})\cos(\omega_a t + \phi)$$

$$+ \varepsilon^{-\frac{\omega_a t}{2Q}}[\cos\phi\cos\omega_a t - \frac{q_N(0)}{QC_N E_a}\sin\omega_a t]\} \qquad \text{(A-20)}$$

Since it is generally more convenient to express an equation in terms of voltage rather than charge, (A-17) may be revised using the transformation $v_N = q_N/C_N$, that is,

$$\frac{V_N(t)}{E_a} = Q\{(1 - \varepsilon^{-\frac{\omega_a t}{2Q}})\sin(\omega_a t + \phi) + \varepsilon^{-\frac{\omega_a t}{2Q}}[\frac{q_N(0)}{QC_N E_a}\cos\omega_a t$$

$$+ (\cos\phi - \frac{1}{2Q}\sin\phi + \frac{1}{2Q^2}\frac{q_N(0)}{C_N E_a})\sin\omega_a t]\} \qquad \text{(A-21)}$$

If the losses in the charging circuit can be neglected then the expression for the charging current, equation (A-20), can be further simplified. This is done by taking the limit of $i_c(t)$ as R_c approaches zero. After application of L'Hospital's Rule (A-20) becomes

$$i_c(t) = \frac{E_a t}{2L_c} \cos(\omega_a t + \phi) + i_c(0)\cos\omega_a t$$

$$+ \left[\frac{E_a}{2L_c\omega_a} \cos\phi - \omega_a\, q_N(0)\right]\sin\omega_a t \qquad \text{(A-22)}$$

Thus, for half cycle charging

$$i_c(\pi) = -\left[\frac{E_a \pi}{2\omega_a L_c} \cos\phi + i_c(0)\right] \qquad \text{(A-23)}$$

As stated earlier, the condition for repeating transients is $i_c(\pi) = - i_c(0)$. Therefore, the only solution for (A-23) is

$$\cos\phi = 0 \text{ or } \phi = \pm\frac{\pi}{2}$$

and so, from (A-15)

$$i_c(0) = 0$$

Equation (A-21) may be evaluated at the discharge point, $\omega_a t = \pi$, to determine the resulting stepup voltage ratio

$$\frac{v_N(\pi)}{E_a} = -\left[Q(1 - \varepsilon^{-\frac{\pi}{2Q}})\sin\phi + \frac{q_N(0)}{C_N E_a}\varepsilon^{-\frac{\pi}{2Q}}\right] \qquad \text{(A-24)}$$

If $\pi/2Q << 1$ then the exponentials in the above equation may be approximated using

$$\varepsilon^{-\frac{\pi}{2Q}} \approx 1 - \frac{\pi}{2Q}$$

and

$$1 - \varepsilon^{-\frac{\pi}{2Q}} \approx \frac{\pi}{2Q}\left(1 - \frac{\pi}{4Q}\right)$$

Substitution of these expressions into (A-24) yields

$$\frac{v_N(\pi)}{E_a} \approx -\left[\frac{\pi}{2}\left(1 - \frac{\pi}{4Q}\right)\sin\phi + \frac{q_N(0)}{C_N E_a}\left(1 - \frac{\pi}{2Q}\right)\right] \qquad \text{(A-25)}$$

Then for the case where there is no initial charge on the network and the losses are negligible, (A-25) becomes

$$\frac{v_N(\pi)}{E_a} \approx -\frac{\pi}{2}\sin\phi \qquad \text{(A-26)}$$

and, thus, for maximum network voltage

$$\phi = -\frac{\pi}{2} \qquad \text{(A-27)}$$

Appendix B

Program EQUATE

PROGRAM EQUATE

```
100=C  THIS PROGRAM INCLUDES THE EQUATIONS FOR THE CHARGING VOLTAGE
110=C  AND CURRENT AT RESONANCE.  THE SOURCE FOR THE EQUATIONS IS THE
120=C  PULSE GENERATOR TEXT BY GLASOE AND LEBACQZ.  FOR COMPARISON
130=C  PURPOSES THE SOURCE AND INDUCTOR VOLTAGE EQUATIONS HAVE ALSO
140=C BEEN INCLUDED.  THE TIME STEP FOR THE EQUATIONS HAS BEEN SET TO
150=C  10.0E-6.  THE EQUATIONS ARE SOLVED AT THESE TIME POINTS FOR
160=C  A HALF PERIOD.  RATHER THAN DISPLAYING THE OUTPUT ON THE
170=C  SCREEN,  IT IS STORED ON TAPE8.
180=C
190=C
200=C
210=       PROGRAM GLASOE(INPUT,OUTPUT,TAPE5=INPUT,TAPE6=OUTPUT,TAPE8)
220=       REAL LC,IC,ICMAX
230=       REWIND 8
240=       PI=3.141592654
250=       RC=0.445
260=       LC=0.858E-3
270=       CN=147.17E-6
280=       EA=150.0
290=       VCZERO=-5.4
300=       PHI=-PI/2.0
310=       A=RC/(2.0*LC)
320=       OMEGA0=1.0/SQRT(LC*CN)
330=       OMEGAA=SQRT(OMEGA0**2-A**2)
340=       RPM=OMEGAA/(0.4*PI)
350=       Q=OMEGAA*LC/RC
360=       QCZERO=CN*VCZERO
370=       FINTIM=PI/OMEGAA
380=       T=0.0
390=       WRITE(6,3)
400=   3   FORMAT(6X,4HTIME,9X,2HIC,12X,2HVC,10X,2HVL,10X,6HOMEGAA)
410= 1     EX=EXP(-OMEGAA*T/(2.0*Q))
420=       IC=Q*CN*EA*OMEGAA*((1.0-EX)*COS(OMEGAA*T+PHI)
430=      #+EX*(COS(PHI)*COS(OMEGAA*T)
440=      #-(QCZERO/(Q*CN*EA)*(1.0-1.0/(4.0*Q**2))
450=      #-1.0/(4.0*Q**2)*SIN(PHI))*SIN(OMEGAA*T)))
460=       VC=EA*Q*((1.0-EX)*SIN(OMEGAA*T+PHI)+EX*
470=      #(QCZERO/(Q*CN*EA)*COS(OMEGAA*T)+
480=      #(COS(PHI)-1.0/(2.0*Q)*SIN(PHI)+1.0/(2.0*Q**2)*
490=      #QCZERO/(CN*EA))*SIN(OMEGAA*T)))
500=       V=EA*COS(OMEGAA*T+PHI)
510=       VL=V-RC*IC-VC
```

```
520=       WRITE(8,2)T,IC,VC,VL,OMEGAA
530=C      WRITE(6,2)T,IC,VC,VL,OMEGAA
540= 2     FORMAT(1X,E12.5,1X,E12.5,1X,E12.5,1X,E12.5,1X,E12.5)
550= 4     ICMAX=IC
560= 5     T=T+10.0E-6
570=       IF(T.LE.FINTIM)GO TO 1
580=       REWIND 8
590=       STOP
600=       END
```

Appendix C

Operating Instructions and Listing for Program RKFOUR

Program RLCCHG

Program RLCDIS

Operating Instructions for RKFOUR

Programmer: B. D. Weathers

Purpose: RKFOUR is an integration routine designed to provide the equivalent of an analog computer integrator for the solution of normal-form differential equations.

Features

---- An arbitrary number of integrators can be used. The number used is determined by the size of the storage arrays set in the calling program.

---- All variables that affect the operation of RKFOUR appear in the calling statement; multiple uses of the program are possible, but care must be used to prevent time desynchronization.

---- The independent variable step size is determined automatically, but if desired this program can be made to run with a fixed step size.

---- The adaptive step size feature, if used, will insure little trouble with numerical instability.

---- The limits on the adaptive step size may be set in the calling program, or default values may be used.

---- The error limits that determine when the step size should be changed are program parameters, and hence may be externally controlled.

---- An adjustable delay is available to prevent eratic step size changing. Once the criteria is satisfied step size increases by the appropriate factor at each time.

---- Step sizes may be changed externally, but may not be changed in the middle of an iteration, that is when KEEP is equal to 0.

A solution point counter is contained in the routine to enable termination if appropriate independent variable criteria is not available.

Suggestions for Use

Before using this subroutine for the first time, a careful examination of the flow chart should be made. Also a thorough examination of the program parameter should be carried out to insure that the default values of the parameters will be satisfactory, if used.

You must set all non-zero initial integrator outputs. All non-unity integrator gains must also be set in section 2.

The value for H(1) - Step Size - should be set as close to the predicted sampling interval as possible. This will insure a more efficient operation for the first pass.

If running in "Open Shop" and the 20 second time limit is just a "bit too short," add "RUN=NO CHECK" to the control card. Do this only after your name, after you are SURE the program is free of programming errors. On a large job this can add 15% to the available computation time, by eliminating several compiler tests.

CALL RKFOUR (NINT, Y, X, GA, PE, XX, H, ZZ1, ZZ2, ZZ3, TIME, PNTS, KEEP, IFL)

NINT - Number of integrators. Storage for the integrators must be defined in the calling program. There is no maximum, but the example program is set for up to 20.

Y - An array that contains the integrator output. Default initial values are zero.

X - An array that contains the integrator inputs.

GA - An array that contains constant gains associated with each integrator. Default values are 1.0.

PE - A working array used to store absolute peak values of the integrator outputs. This array is set to zero during initial entry to RKFOUR.

XX - An array used in two ways. If I denotes the Ith integrator, then XX(1,I) stores the past value of the integrator output and XX(2,I) stores the past value of the integrator input. During the integration cycle the XX(3,I) and XX(4,I) positions are used to store the derivative values needed by the integration algorithm. At the end of a cycle, XX(3,I) holds the new integrator output and XX(4,I) holds the new integrator input. It is possible, with the values, to implement a third order interpretation for the values of the integrator outputs between steps. This would serve to offset the problem of obtaining values at discrete time points and would be more efficient than step size manipulation.

H Array - The integration control parameters.

H (1) - The current independent variable step size.

H (2) - Minimum permissible step size (Default value is 0.0).

H (3) - Maximum step size (Default value is 1.0E + 8).

H (4) - Factor used to modify the step size—must be greater than 1.0 (Default value is SQRT of 2=1.414214).

H (5) - Proportional to the lower error bound (Default value is 1.0E - 4).

H (6) - Proportional upper error bound (Default value is 1.0E - 02).

H (7) - Adaptive step size control (Set to -1 for constant step size operation) (Default value of 0.0 causes adaptive step size operation).

H (8) - Delay in increasing the step size after error criteria is met. (Default value is 3.0).

H (9) - Last value of the independent variable.

ZZ1, ZZ2, ZZ3 - Working arrays used to store the constants needed for the integration routine. These arrays are

TIME - The independent variable set within RKFOUR. The default initial value is zero.

PNTS - The counter of permanent solution extensions. Use this variable for termination when other termination options fail.

KEEP - This variable is set to ONE only when the data in the derivative evaluation section is permanent. It is zero at all other times. This variable should be used as a control upon memory dependent functions.

IFL - The IFLag array.

IFL(1) - Set to -1 at the first entry to RKFOUR, and is 0 at the first exit. On subsequent exits it has a value +1.

IFL(2) - Has the value -1 to +3 depending upon where the integration routine is in its operation cycle.

IFL(3) - This flag is used to control the step size from the derivative evaluation section of the calling program. It is set to -1 for step size reduction, and +1 for an increase in the step size.

IFL(4) - This flag is -1 when initializing calculations are to

be made. It is 0 when only the derivative evaluation is required, and is +1 when the solution has been successfully extended over one step of the independent variable.

IFL(5) - This flag is set to +1 immediately after IFL(4) is -1 for the first time. It is intended as a signal for other routines that may be used that initialization is underway.

IFL(6) - This flag is used for the temporary storage of the variable KEEP.

The Basic RKFOUR Program

```
      DIMENSION Y(20)4, X(20)4, GA(20)4, PE(20), XX(4,20), H(9)
      DIMENSION ZZ1(20), ZZ2(20), ZZ3(20), IFL(7)
```

If Other Dimensioned Variables are required the necessary DIMENSION statements go here.

SECTION 1 INSERTIONS GO HERE

```
      NRUN = (Number of runs to be made)
      DO 6 IRUN=1,NRUN
      ISTOP=0
      KEEP=1
      IFL(1)=-1
      NINT=(Number of integrators required)
    1 IFL(2)=-1
    2 CALL RKFOUR(NINT,Y,X,GA,PE,XX,H,ZZ1,ZZ2,ZZ3,TIME,PNTS,KEEP,IFL)
      IF (IFL[4])3,4,5
    3 INT=1
      TIME1=-1.256789
      NC=1
      NCC=1 (Portion of Points released to Section 5)
      FINTIM= (Maximum Value for TIME in this run)
      PTMAX= (Maximum Number of solution points for this run)
```

SECTION 2 INSERTIONS GO HERE

```
    4 IF(TIME - TIME1)7,8,9
    7 TIME1=TIME
```

SECTION 3 INSERTIONS GO HERE

```
    8 CONTINUE
```

SECTION 4 INSERTIONS GO HERE (Exclude everything nonessential)

```
        GO TO 2
    5 IPR=0
      NC=NC-1
      IF (NC)9,9,10
    9 NC=NCC
      IPR=1
   10 IF(TIME.GE.FINTIM.OR.PNTS.GE.PTMAX) ISTOP=1
      IF ([IPR+ISTOP].EQ.0) GO TO 11
```

```
SECTION 5 INSERTIONS GO HERE

 11  INIT=0
     IF (ISTOP)1,1,6
  6  CONTINUE
     WRITE (6,100)
100  FORMAT (1H1, 1X)
     STOP
     END
```

Basic RKFOUR System

There are a number of variables in the RKFOUR System whose value depends upon the problem undertaken.

NRUN - The number of runs to be made.

NINT - The number of integrators to be used in the run (limited to 20 by storage allocation in the stock system).

NCC - The portion of solution points that are released to the output section (Section 5) NCC = 1 delivers every point, NCC = 2, every second point, etc.

FINTIM - The maximum value that the independent variable will attain. The program will terminate upon the first solution point to meet or exceed this value.

PTMAX - The maximum number of solution points in any one run.

IPNT - The point counter used in plot routines. It may be set to 0 in one of two locations. If summary curves are desired, set to 0, before the IRUN DO statement. If no curves are desired, set to 0 after the IRUN DO statement.

INIT - This variable is 1 the first interation step, and 0 thereafter. This can be used as a memory flag for memory dependent functions.

The Basic RKFOUR System contains five sections where the particular problem statements may be inserted.

1. This section is used to initialize those values which are not run dependent, or whose calculation in block form is more efficient. In this case they may be indexed by IRUN for use in the rest of the program.
2. This section is used to:
   a. Set non-zero integrators initial conditions
   b. Set non-unity integrator gains
   c. Override any default values set by RKFOUR subroutine
   d. Carry out calculations that are run dependent and need be carried out only once per run
3. This section is used to carry out all calculations of the functions of the independent variable.
4. This section contains the derivative evaluation equations. It is executed four times for each point and should be carefully structured. For example:

   X(1)=(A+B)/(D+E) + U(1)*(G+H) would be efficiently written as

   X(1) = AB + Y(1) * GH

   where AB = (A+B)/(D+E)

   GH = G + H

   and are evaluated in section 1,2, or 3 as is appropriate.
5. This section is used to call the output routines. If NCC is not equal to 1 it is not entered on every pass, and this should be considered when structuring the problem.

SUBROUTINE RKFOUR

```
  100=      SUBROUTINE RKFOUR(N,Y,X,GAIN,PEAK,XX,H,C1,C2,C3,TIME,PNTS,K
EEP,FL)
  110=      DIMENSION Y(20),X(20),GAIN(20),PEAK(20),XX(4,20),
  120=     $H(9),C1(20),C2(20),C3(20),A(8)
  130=      INTEGER FL(7)
  140=      DATA A(1)/0.1/,A(2)/0.0/,A(3)/1.0E8/,A(4)/1.414214/,A(5)/1.
03E-4/
  150=      DATA  A(6)/1.0E-2/,A(7)/0.0/,A(8)/3.0/
  160=C
  170=      IF(FL(1)) 1,3,20
  180=1     DO 2 I=1,N
  190=      Y(I)=0.0
  200=      PEAK(I)=0.0
  210=2     GAIN(I)=1.0
  220=      TIME=0.0
  230=      PNTS=0.0
  240=      FL(4)=-1
  250=      FL(5)=1
  260=      FL(1)=0
  270=      DO 9 I= 1,8
  280=9     H(I)=A(I)
  290=       RETURN
  300=3     Q=H(1)
  310=      FL(4)=1
  320=      FL(7)=H(8)
  330=4     H(1)=Q
  340=      FL(3)=0
  350=      DO 5 I=1,N
  360=      C2(I)=GAIN(I)*Q
  370=      C1(I)=0.5*C2(I)
  380=5     C3(I)=C2(I)/6.0
  390=      IF(FL(1)) 6,6,10
  400=10     IF(FL(2)) 31,33,33
  410=6     FL(1)=1
  420=7     PNTS=PNTS+1.0
  430=      DO 8 I=1,N
  440=      XX(3,I)=Y(I)
  450=8     XX(4,I)=X(I)
  460=      FL(4)=1
  470=      H(9)=TIME
  480=       RETURN
  490=20    IF(FL(3)) 25,30,25
  500=25    IF(FL(2)-3) 26,60,60
  510=26    IF(FL(3)) 21,30,22
  520=21    Q=H(1)/H(4)
  530=      IF(Q-H(2)) 23,4,4
  540=23    Q=H(2)
  550=      IF(Q-H(1)) 4,30,4
  560=22     Q=H(1)*H(4)
  570=      IF(Q-H(3)) 4,4,24
  580=24    Q=H(3)
```

```
590=      IF(Q-H(1)) 4,30,4
600=30    FL(5)=0
610=      IF(FL(2)) 31,40,45
620=31    FL(6)=KEEP
630=      KEEP=0
640=      DO 32 I=1,N
650=      XX(1,I)=XX(3,I)
660=32    XX(2,I)=XX(4,I)
670=33    FL(2)=0
680=      TIME= H(9)+0.5*H(1)
690=      DO 34 I=1,N
700=34    Y(I)=XX(1,I)+C1(I)*XX(2,I)
710=35    KEEP = 0
720=36    FL(4)=0
730=       RETURN
740=40    FL(2)=1
750=      DO 41 I=1,N
760=      XX(3,I)=X(I)
770=41    Y(I)=XX(1,I)+C1(I)*X(I)
780=      GO TO 35
790=45    IF(FL(2)-2) 46,48,60
800=46    FL(2)=2
810=      TIME=H(9)+H(1)
820=      DO 47 I=1,N
830=      XX(4,I)=X(I)
840=47    Y(I)=XX(1,I)+C2(I)*X(I)
850=      GO TO 35
860=48    FL(2)=3
870=      IF(H(7)) 49,52,52
880=49      KEEP=FL(6)
890=50    DO 51 I=1,N
900=51    Y(I)=XX(1,I)+C3(I)*(XX(2,I)+X(I)+2.*(XX(3,I)+XX(4,I)))
910=      GO TO 36
920=52    ERR=0.0
930=       DO 56  I=1,N
940=      ESTERR= C2(I)*ABS(XX(2,I)+X(I)-2.*XX(4,I))
950=      IF(PEAK(I)) 53,53,54
960=54    ESTERR=ESTERR/PEAK(I)
970=53    IF(ERR-ESTERR) 55,56,56
980=55    ERR=ESTERR
990=56     CONTINUE
```

```
1000=       IF(ERR-H(6)) 57,57,66
1010=57     IF(ERR-H(5)) 58,59,59
1020=58     FL(7)=FL(7)-1
1030=       IF(FL(7)) 65,65,49
1040=65     FL(3)=1
1050=       GO TO 49
1060=59     FL(7)=H(8)
1070=       GO TO 49
1080=66     FL(7)=H(8)
1090=       GO TO 21
1100=60     IF(H(7)) 7,61,61
1110=61     DO 63 I=1,N
1120=       ERR=ABS(Y(I))
1130=       IF(ERR-PEAK(I)) 63,63,62
1140=62     PEAK(I)=ERR
1150=63     CONTINUE
1160=       GO TO 7
1170=       END
```

PROGRAM RLCCHG

```
100=C  THIS PROGRAM USES THE RKFOUR SUBROUTINE TO INTEGRATE THE
110=C  DIFFERENTIAL EQUATIONS OF AN RLC CIRCUIT WITH A SINUSOIDAL
120=C  INPUT AND AN INITIAL VOLTAGE ON THE CAPACITOR.  THE CHARGING
130=C  CURRENT, CHARGING VOLTAGE, AND INDUCTOR VOLTAGE ARE EACH
140=C  CALCULATED AND WRITTEN TO TAPE8 WHERE THEY MAY BE EDITED
150=C  AND VIEWED.  THE INTEGRATION TIME IS OVER A HALF CYCLE.
160=C
170=C
180=C
190=       PROGRAM RLCCHG(INPUT,OUTPUT,TAPE5=INPUT,TAPE6=OUTPUT,TAPE8)
200=       DIMENSION Y(20),X(20),GA(20),PE(20),XX(4,20),H(9)
210=       DIMENSION ZZ1(20),ZZ2(20),ZZ3(20),IFL(7)
220=       REAL I,L,LA
230=C      SECTION 1 INSERTIONS ********************************
240=       R=0.445
250=       L=0.858E-3
260=       C=147.17E-6
270=       PI=3.1415927
280=       EA=250.0
290=       A=R/(2.0*L)
300=       OMEGA0=1.0/SQRT(L*C)
310=       OMEGAA=SQRT(OMEGA0**2-A**2)
320=C      IPNT=0 HERE IF SUMMARY CURVES ARE DESIRED
330=C      NRUN=
340=       NRUN=1
350=       DO 6 IRUN=1,NRUN
360=       IPNT= 0
370=       WRITE(6,100)
380=       ISTOP=0
390=       KEEP=1
400=       IFL(1)=-1
410=C      NINT= NUMBER OF INTEGRATORS
420=       NINT=2
430= 1     IFL(2)=-1
440= 2     CALL RKFOUR(NINT,Y,X,GA,PE,XX,H,ZZ1,ZZ2,ZZ3,TIME,PNTS,KEEP,
IFL)
450=       IF(IFL(4))3,4,5
460= 3     INIT=1
470=       TIME1=-1.256789
480=       NC=1
490=       NCC=1
500=C      NCC=NUMBER OF POINTS KEPT
510=C      FINTIM=FINISH TIME
520=       FINTIM=PI/OMEGAA
530=C      PTMAX=MAXIMUM NUMBER OF POINTS
540=       PTMAX=800
```

```
550=C     SECTION 2 INSERTIONS   ************************************
560=      Y(1)=-5.4
570=      H(1)=1.0E-07
580=      GA(1)=1.0/C
590=      GA(2)=1.0/L
600=      WRITE(6,101)
610= 4    IF(TIME-TIME1)7,8,7
620= 7    TIME1=TIME
630=C     SECTION 3 INSERTIONS  ****************************
640=      V=EA*SIN(OMEGAA*TIME)
650= 8    CONTINUE
660=C     SECTION 4 INSERTIONS   *******************************
670=      VR=Y(2)*R
680=      VL=V-VR-Y(1)
690=      X(2)=VL
700=      X(1)=Y(2)
710=      I=Y(2)
720=      VC=Y(1)
730=      GO TO 2
740= 5    IPR=0
750=      NC=NC-1
760=      IF(NC)9,9,10
770= 9    NC=NCC
780=      IPR=1
790= 10   IF(TIME.GE.FINTIM.OR.PNTS.GE.PTMAX)ISTOP=1
800=      IF((IPR+ISTOP).EQ.0)GO TO 11
810=C     SECTION 5 INSERTIONS  ********************************
820=      WRITE(8,102)TIME,I,VC,VL
830=C     WRITE(6,102)TIME,I,VC,VL
840= 11   INIT=0
850=      IF(ISTOP)1,1,6
860= 6    CONTINUE
870=      WRITE(6,100)
880= 100  FORMAT(1H1,1X)
890=  101 FORMAT(7X,4HTIME,13X,2HIC,13X,2HVC,13X,2HVL)
900= 102  FORMAT(2X,E12.5,3X,E12.5,3X,E12.5,3X,E12.5)
910=      END FILE 8
920=      STOP
930=      END
```

PROGRAM PLCDIS

```
100=C  THIS PROGRAM USES THE RKFOUR SUBROUTINE TO INTEGRATE THE
110=C  DIFFERENTIAL EQUATIONS IN AN RLC DISCHARGE LOOP.  THE SOURCE
120=C  VOLTAGE IS SET TO ZERO AND THE CAPACITOR IS CHARGED TO AN
130=C  INITIAL VALUE.  THE INITIAL CURRENT IS SET TO ZERO.
140=C  THE OUTPUT IS READ TO TAPE8 WHICH MAY THEN BE EDITED FOR
150=C  GRAPHING OR VIEWING.  THE  TIME AT WHICH INTEGRATION CEASES IS
160=C  DEPENDENT UPON THE DAMPED RESONANT FREQUENCY OF THE CIRCUIT.
170=C
180=C
190=C
200=       PROGRAM PLCDIS(INPUT,OUTPUT,TAPE5=INPUT,TAPE6=OUTPUT,TAPE8)
210=       DIMENSION Y(20),X(20),GA(20),PE(20),XX(4,20),H(9)
220=       DIMENSION ZZ1(20),ZZ2(20),ZZ3(20),IFL(7)
230=       REAL I,L
240=C      SECTION 1 INSERTIONS ********************************
250=       R=11.0
260=       L=29.0E-6
270=       C=0.43E-6
280=       PI=3.1415927
290=       A=R/(2.0*L)
300=       OMEGA0=1.0/SQRT(L*C)
310=       OMEGAA=SQRT(OMEGA0**2-A**2)
320=C      IPNT=0 HERE IF SUMMARY CURVES ARE DESIRED
330=C      NRUN=
340=       NRUN=1
350=       DO 6 IRUN=1, NRUN
360=       IPNT= 0
370=       WRITE(6,100)
380=       ISTOP=0
390=       KEEP=1
400=       IFL(1)=-1
410=C      NINT= NUMBER OF INTEGRATORS
420=       NINT=2
430= 1     IFL(2)=-1
440= 2     CALL RKFOUR(NINT,Y,X,GA,PE,XX,H,ZZ1,ZZ2,ZZ3,TIME,PNTS,KEEP,
450=      *IFL)
460=       IF(IFL(4))3,4,5
470= 3     INIT=1
480=       TIME1=-1.256789
490=       NC=1
500=       NCC=1
510=C      NCC=NUMBER OF POINTS KEPT
520=C      FINTIM=FINISH TIME
530=       FINTIM=PI/OMEGAA
540=C      PTMAX=MAXIMUM NUMBER OF POINTS
550=       PTMAX=800
```

```
560=C     SECTION 2 INSERTIONS   ********************************
570=      Y(1)=-6000.0
580=      H(1)=1.0E-07
590=      GA(1)=1.0/C
600=      GA(2)=1.0/L
610=      WRITE(6,101)
620= 4    IF(TIME-TIME1)7,8,7
630= 7    TIME1=TIME
640=C     SECTION 3 INSERTIONS  ****************************
650=      V=0.0
660= 3    CONTINUE
670=C     SECTION 4 INSERTIONS   ********************************
680=      VR=Y(2)*R
690=      VL=V-VR-Y(1)
700=      X(2)=VL
710=      X(1)=Y(2)
720=      I=Y(2)
730=      VC=Y(1)
740=      GO TO 2
750= 5    IPR=0
760=      NC=NC-1
770=      IF(NC)9,9,10
780= 9    NC=NCC
790=      IPR=1
800= 10   IF(TIME.GE.FINTIM.OR.PNTS.GE.PTMAX)ISTOP=1
810=      IF((IPR+ISTOP).EQ.0)GO TO 11
820=C     SECTION 5 INSERTIONS  ********************************
830=      WRITE(8,102)TIME,I,VC,VL
840=C     WRITE(6,102)TIME,I,VC,VL
850=C     CALL FPLOT(800,IPNT,AR,LR,0,1,2,TIME,V)
860=C     CALL FPLOT(800,IPNT,AR,LR,ISTOP,2,2,TIME,VC)
870= 11   INIT=0
880=      IF(ISTOP)1,1,6
890= 6    CONTINUE
900=      WRITE(6,100)
910= 100  FORMAT(1H1,1X)
920=  101 FORMAT(7X,4HTIME,13X,2HIC,13X,2HVC,13X,2HVL)
930= 102  FORMAT(2X,E12.5,3X,E12.5,3X,E12.5,3X,E12.5)
940=      END FILE 8
950=      STOP
960=      END
```

Appendix D

Equipment List

Alternator - 3 phase, 4 wire, 24 pole

Model LPL-72-2450

S/N 711941-0007

18.8 KVA, 15 KW @ 0.8 pf lagging

120/208 volts, 52 amps

240/416 volts, 26 amps

400 Hertz, 2000 RPM

X_{ℓ} = 0.0594 pu

X_{ad} = 0.456 pu

X_{aq} = 0.265 pu

High Leakage Transformers (3)

Electro Type E 18230; S/N 1, 2, and 3

19.98 KVA, 400 Hertz, Single phase

Terminals 1-2: 240 volts, 84 amps

Terminals 3-4: 4440 NL, 4.5 amps

DC Power Supply (Exciter Field Excitation)

HP Model 62928

Instrumentation

7834 Storage Oscilloscope - Tektronix with HV probes

Ammeters - Weston Model 433

Wattmeters - Westinghouse S/N 32982/32983/32984

Digital Multimeter (True RMS) - HP Model 3466A, S/N 24885

Thyratrons - JAN 8613, 5 MW Peak Power

20 KV Peak Anode Voltage

500 Amps Peak Forward Current

Charging Diodes - Rectifier Stock Built Up of 222K ohm resistors, 0.05 μf capacitors, and 1 KV PRV diodes

30 KV Peak Reverse Voltage

20 Amps Nominal Current

Appendix E

Leakage Transformer Short-Circuit Test

(C Phase Transformer S/N 3)

I_P = 81.6 amps RMS

I_S = 4.5 amps RMS

V_P = 142 volts RMS

P = 950 watts

$R = P/I_P^2 = 0.1427$ ohms

$Z = V_P/I_P = 1.74$ ohms

$X = \text{SQRT}\ (Z^2 - R^2) = 1.734$ ohms

$L = X/[2\pi(400)] = 0.69$ mh

$Z_B = 240/84 = 2.857$

$R_{pu} = R/Z_B = 0.04995$ pu

$X_{pu} = X/Z_B = 0.6069$ pu

Vita

William C. Dungan was born on July 24, 1946 in Lucedale, Mississippi. He graduated from Rocky Creek High School, Lucedale, Mississippi in 1964 and attended Mississippi State University from which he received a Bachelor of Science degree in Electrical Engineering in 1970. He entered the Air Force in July 1972 and was assigned to the Service Engineering Division at the Warner Robins Air Logistics Center, Robins AFB, Georgia. His reassignment to the Air Force Aero Propulsion Laboratory was made in April 1977 where he served as a research and development engineer and as a laboratory staff officer. He then entered the Air Force Institute of Technology, School of Engineering, in June 1980.

Permanent Address: Route 8, Box 165
Lucedale, MS 39452

Unclassified

SECURITY CLASSIFICATION OF THIS PAGE (When Data Entered)

REPORT DOCUMENTATION PAGE	READ INSTRUCTIONS BEFORE COMPLETING FORM
1. REPORT NUMBER: AFIT/GE/EE/81D-18	2. GOVT ACCESSION NO.: AD-A115 551
3. RECIPIENT'S CATALOG NUMBER	
4. TITLE (and Subtitle): AC RESONANT CHARGING FOR INTERFACING PRIME POWER TO PULSE CONDITIONING CIRCUITS	5. TYPE OF REPORT & PERIOD COVERED: MS Thesis
	6. PERFORMING ORG. REPORT NUMBER
7. AUTHOR(s): William C. Dungan, Capt, USAF	8. CONTRACT OR GRANT NUMBER(s)
9. PERFORMING ORGANIZATION NAME AND ADDRESS: School of Engineering, Air Force Institute of Technology (AFIT), Wright-Patterson AFB, OH 45433	10. PROGRAM ELEMENT, PROJECT, TASK AREA & WORK UNIT NUMBERS
11. CONTROLLING OFFICE NAME AND ADDRESS: Electrical Equipment Division, DRDME-EAM, Ft. Belvoir, VA 22060	12. REPORT DATE: December 1981
	13. NUMBER OF PAGES: 86
14. MONITORING AGENCY NAME & ADDRESS (if different from Controlling Office)	15. SECURITY CLASS. (of this report): Unclassified
	15a. DECLASSIFICATION DOWNGRADING SCHEDULE

16. DISTRIBUTION STATEMENT (of this Report)
Approved for public release; distribution unlimited.

17. DISTRIBUTION STATEMENT (of the abstract entered in Block 20, if different from Report)

18. SUPPLEMENTARY NOTES
Approved for public release; IAW AFR 190-17

15 APR 1982

FREDERIC C. LYNCH, ~~Major~~, USAF
~~Director of Public Affairs~~

Lynn E. Wolaver

Dean for Research and Professional Development
Air Force Institute of Technology (ATC)
Wright-Patterson AFB, OH 45433

19. KEY WORDS (Continue on reverse side if necessary and identify by block number)
AC Resonant Charging
DC Resonant Charging
Pulse Power

20. ABSTRACT (Continue on reverse side if necessary and identify by block number)
The impact on a prime power source due to AC resonant charging was investigated. The source was a standard DOD 15 KW, 400 Hz alternator. Adverse impact on the alternator was almost negligible for a varying load of 15 to 60 KW and a frequency change of 380 to 475 Hz. The only exception was caused by the pulser diodes. Their turn-on was reflected in the alternator voltage waveforms. An indirect approach is presented for determining resonance and, thus, the internal reactance contribution by the alternator. This value was found to be slightly less than that specified for the leakage reactance. The investigation concludes that

DD FORM 1 JAN 73 1473 EDITION OF 1 NOV 65 IS OBSOLETE

Unclassified

SECURITY CLASSIFICATION OF THIS PAGE (When Data Entered)

resonance, in the classical steady state sense, is never reached. Even though the charging circuit has a transient response, the alternator armature reaction is approximately fixed. This implies that the alternator is in a near steady state mode of operation.

END

DATE
FILMED

7 82

DTIC